

Sign-problem-free Nuclear Quantum Monte Carlo Simulation

Bing-Nan Lu

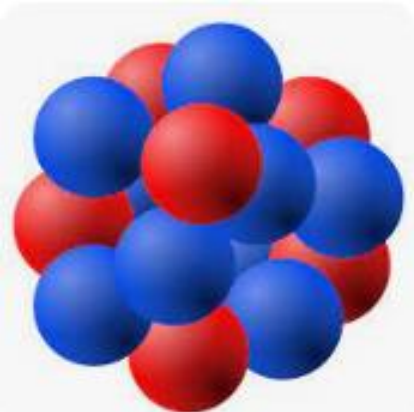
吕炳楠

Graduate School of China Academy of Engineering Physics

中国工程物理研究院研究生院

第二届原子核从头计算与贝塔衰变前沿研讨会

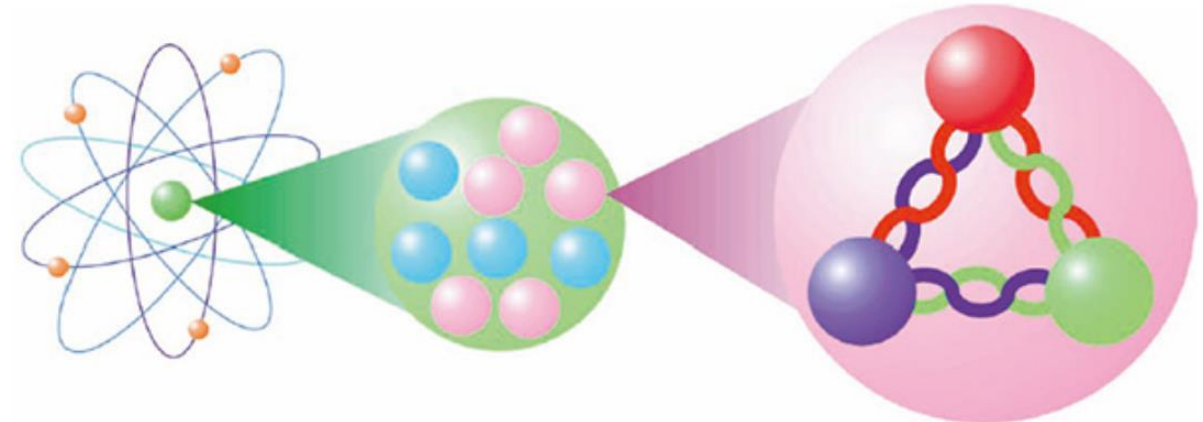
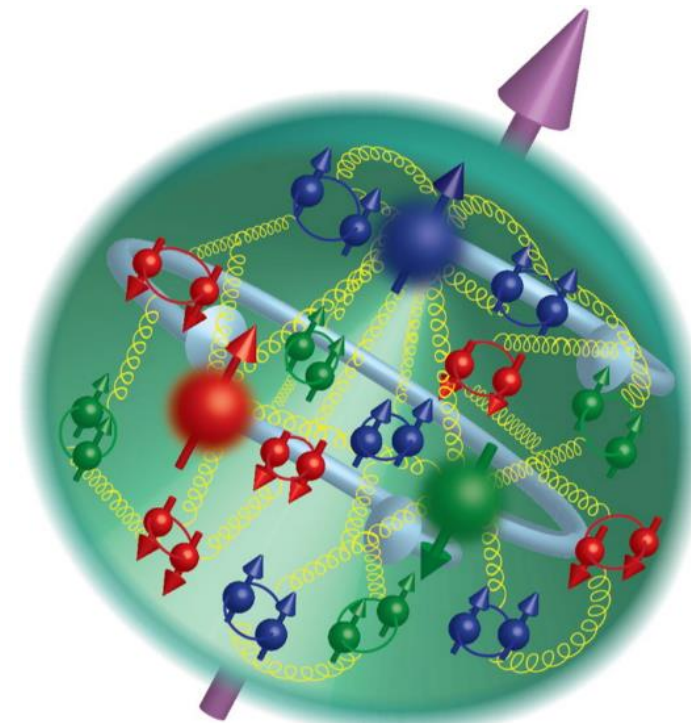
Jan-11, 2026



Hierarchy of strongly interacting systems

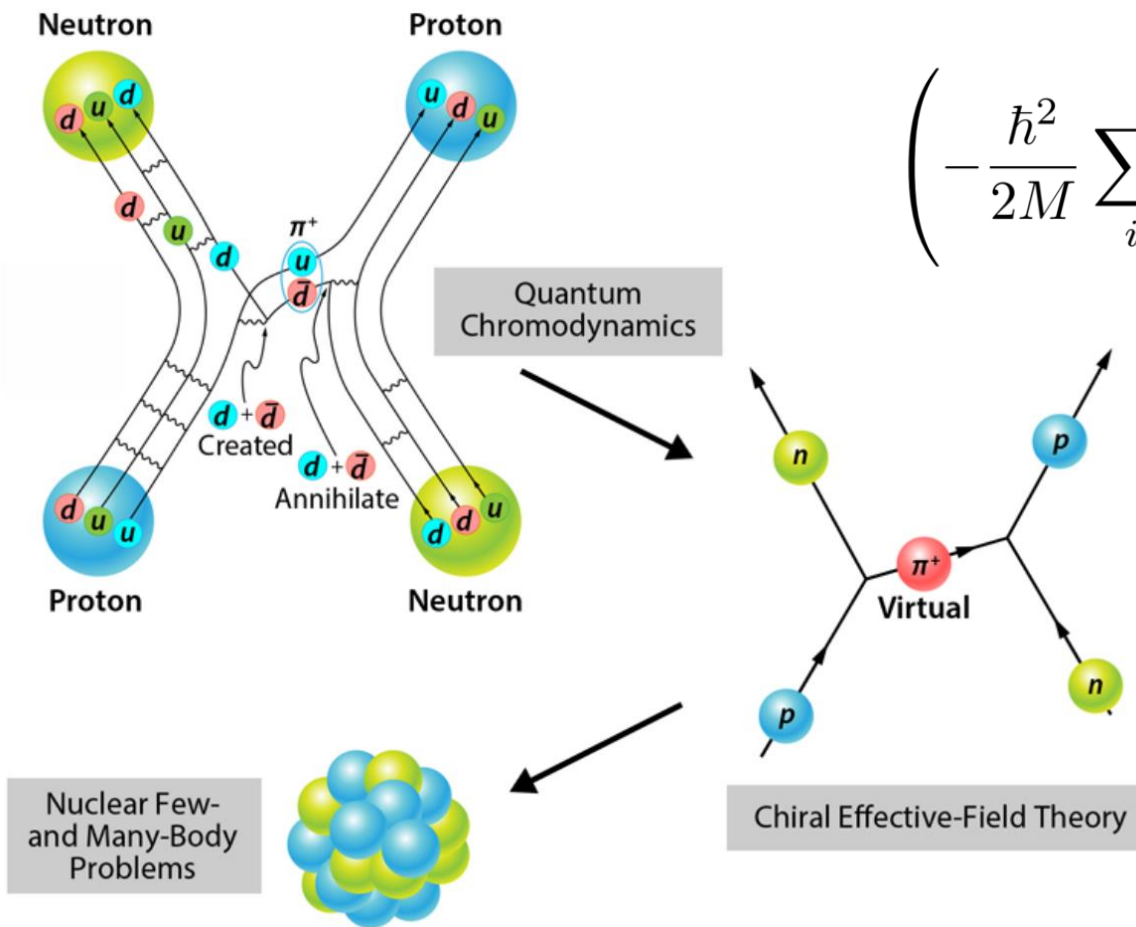
$$\mathcal{L}_{\text{QCD}} = \bar{\psi}_i (i\gamma^\mu (D_\mu)_{ij} - m \delta_{ij}) \psi_j - \frac{1}{4} G_{\mu\nu}^a G_a^{\mu\nu}$$

QCD Quark Confinement



- Quarks are **confined** in nucleons
- Nuclear forces among nucleons are **emergent phenomena**

What is nuclear *ab initio* calculations?



Nuclear forces

$$\left(-\frac{\hbar^2}{2M} \sum_i \nabla_i^2 + \sum_{i < j} V_{ij} + \sum_{i < j < k} V_{ijk} + \dots \right) \Psi = E\Psi$$



Typical nuclear forces

complicated operator structures
emerging from QCD



$$v_{ij} = \sum_{p=1,18} v_p(r_{ij}) O_{ij}^p$$

$O_{ij}^{p=1,14} = \gamma, \tau_i \cdot \tau_j, \sigma_i \cdot \sigma_j, (\sigma_i \cdot \sigma_j)(\tau_i \cdot \tau_j), S_{ij}, S_{ij}(\tau_i \cdot \tau_j), L \cdot S, L \cdot S(\tau_i \cdot \tau_j), L^\gamma, L^\gamma(\tau_i \cdot \tau_j), L^\gamma(\sigma_i \cdot \sigma_j), L^\gamma(\sigma_i \cdot \sigma_j)(\tau_i \cdot \tau_j), (L \cdot S)^\gamma, (L \cdot S)^\gamma(\tau_i \cdot \tau_j),$

CHARGE DEPENDENT

$$O_{ij}^{p=15,17} = T_{ij}, (\sigma_i \cdot \sigma_j) T_{ij}, S_{ij} T_{ij}$$

CHARGE ASYMMETRIC

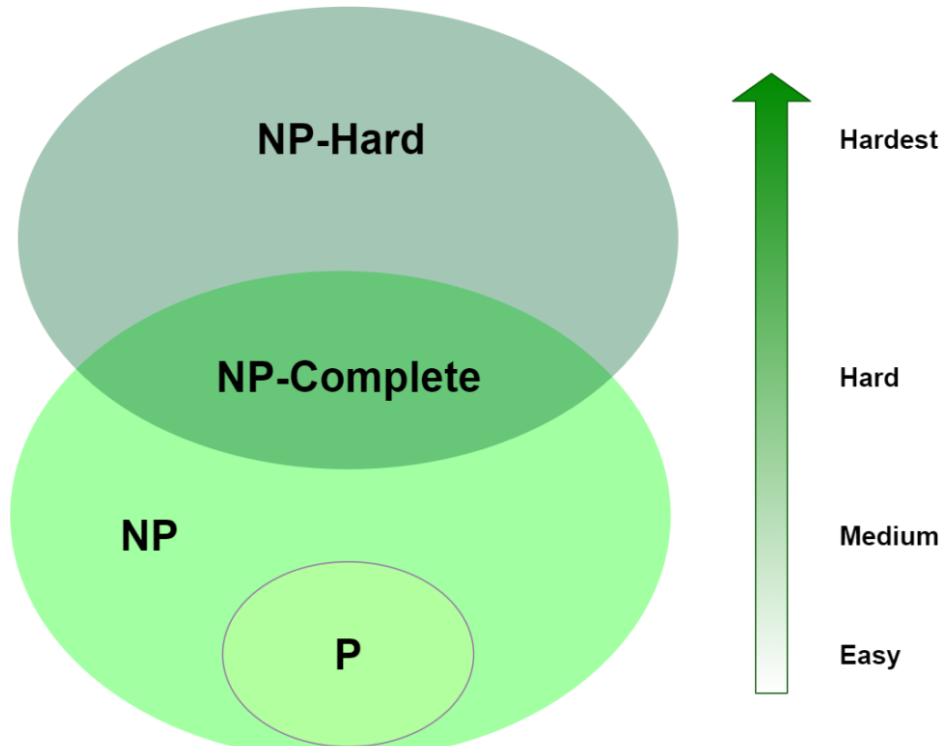
$$O_{ij}^{p=18} = (\tau_{zi} + \tau_{zj})$$

R. B. Wiringa, V. G. J. Stoks, and R. Schiavilla, Phys. Rev. C 51, 38, 1995.

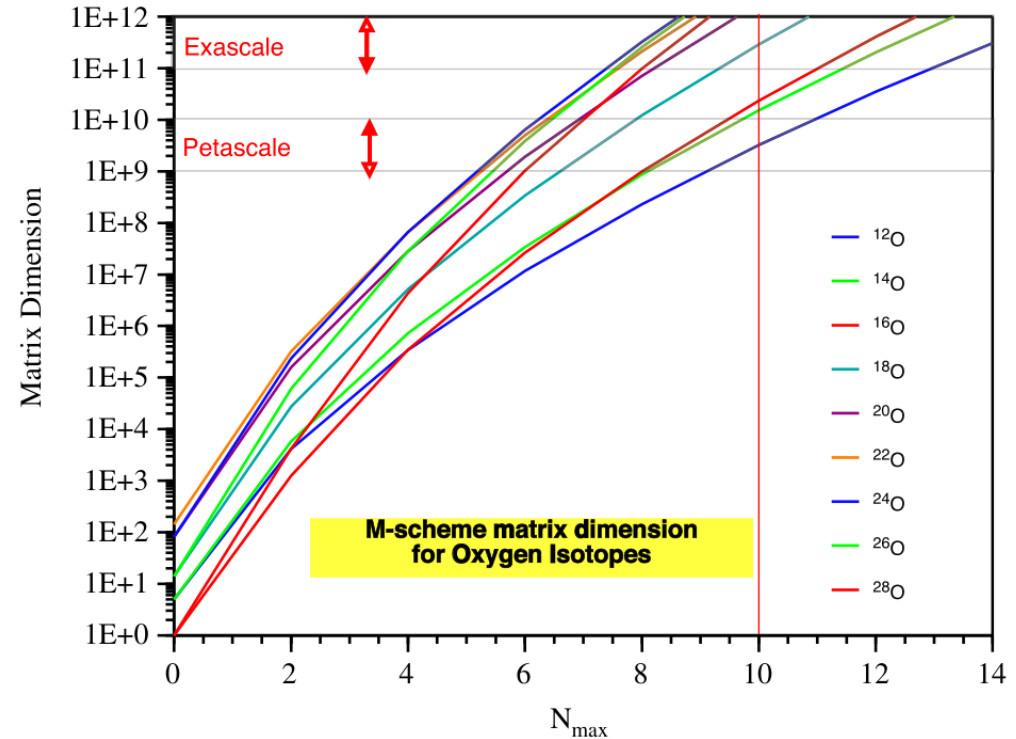
Nuclear chiral EFT

	2N force	3N force	4N force
LO		—	—
NLO		—	—
N ² LO			
N ³ LO		...	

Complexity of nuclear many-body problem



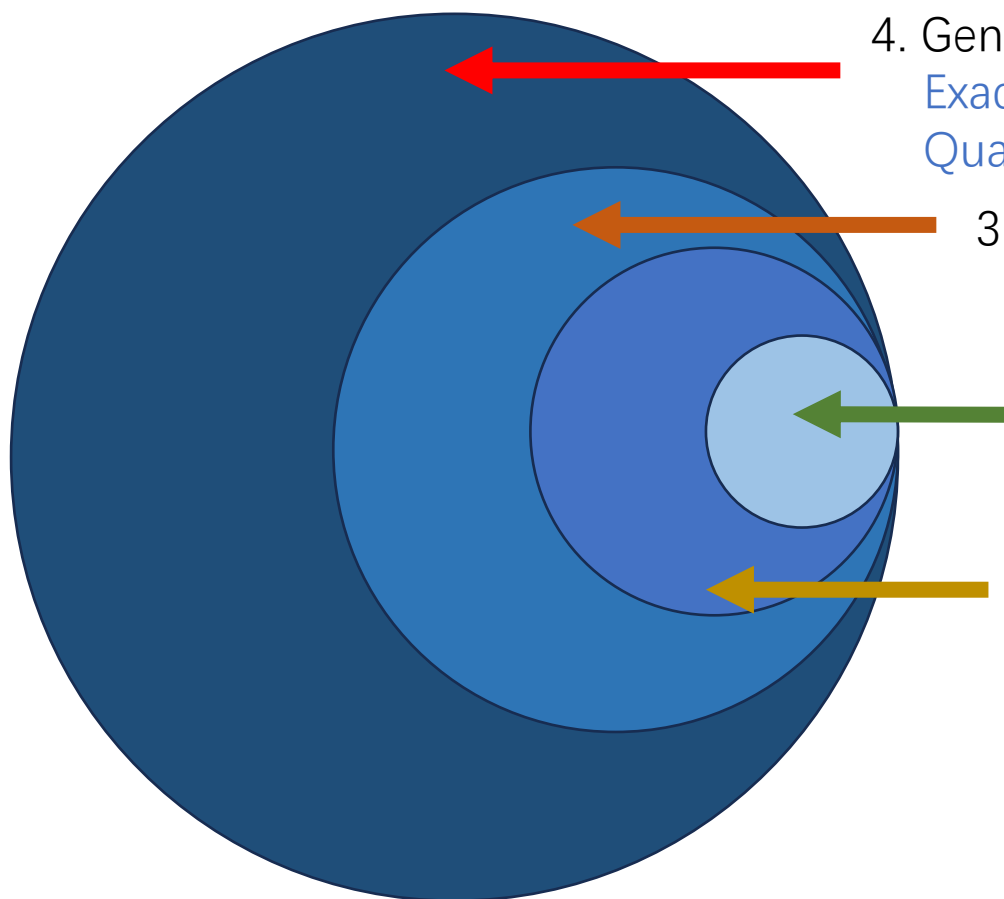
- P: Solvable within polynomial time
- NP: Verifiable within polynomial time



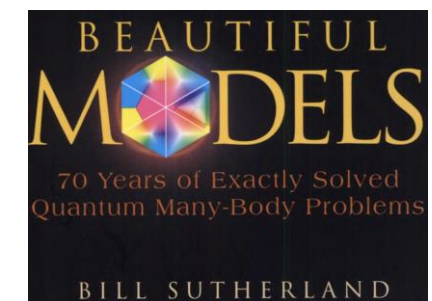
Exponentially increasing Hilbert space
→ **Find ground state of a general Hamiltonian is NP-Hard**

Quantum many-body problem classification

- Models with strong interactions present great challenges



4. General quantum many-body problem (NP-hard)
Exact diagonalization
Quantum computing
3. Problems perturbatively solvable
QMC with sign problem
(Nuclear *ab initio* calculations)
1. Problems analytically solvable
only possible in 1-d systems
2. Problems with polynomial algorithms
QMC without sign problem



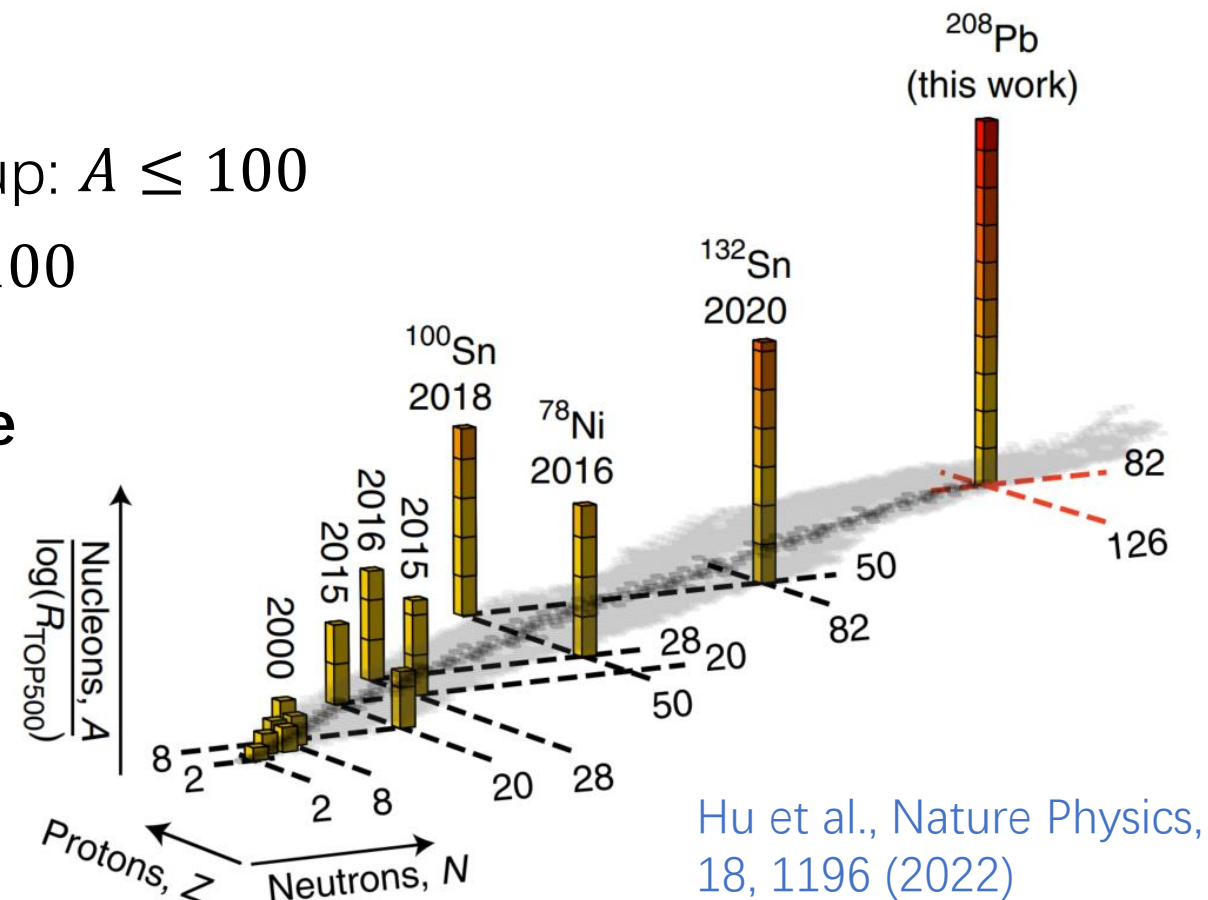
Nuclear *ab initio* algorithms

- No core shell model: $A \leq 20$
- Green's function Monte Carlo: $A \leq 20$
- Coupled cluster: $A \leq 100$
- In-medium similarity renormalization group: $A \leq 100$
- Nuclear lattice effective field theory: $A \leq 100$

Developments of **algorithms** and **hardware**
rapidly push the frontiers of
nuclear *ab initio* calculations

mass / temperature / strangeness /...

Rapid growth in last decade

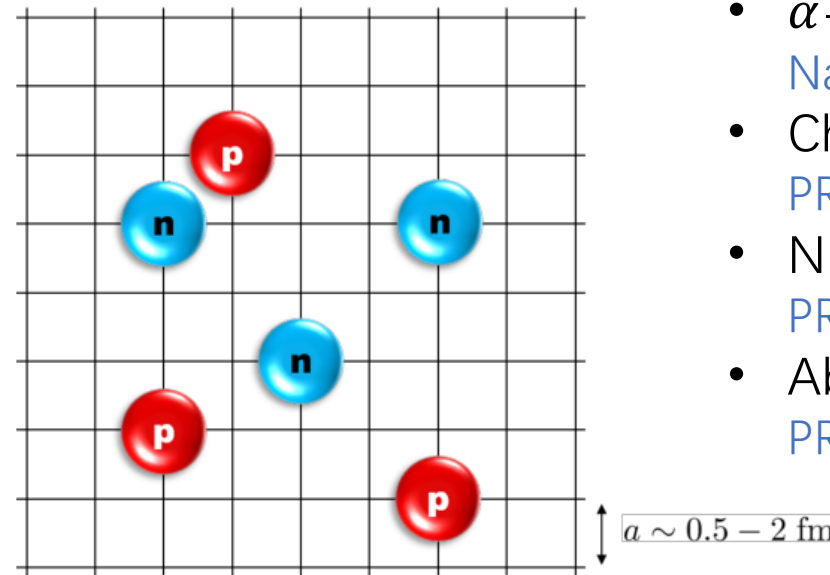


Nuclear Lattice EFT: An efficient nuclear many-body solver

$$\text{Lattice EFT} = \text{Chiral EFT} + \text{Lattice} + \text{Monte Carlo}$$

Review: Dean Lee, Prog. Part. Nucl. Phys. 63, 117 (2009),
Lähde, Meißner, "Nuclear Lattice Effective Field Theory", Springer (2019)

- Discretized **chiral nuclear force**
- Lattice spacing $a \approx 1 \text{ fm} = 620 \text{ MeV}$
(\sim chiral symmetry breaking scale)
- Protons & neutrons interacting via
short-range, δ -like and **long-range,**
pion-exchange interactions
- Exact method, **polynomial scaling** ($\sim A^2$)



Lattice adapted for nucleus

Nature *, PRL > 20

- Hoyle state
[PRL106-192501 \(2011\)](#)
- α - α scattering
[Nature528-111 \(2015\)](#)
- Charge distribution
[PRL119-222505 \(2017\)](#)
- Nuclear thermodynamics
[PRL125-192502 \(2020\)](#)
- Ab initio ^{100}Sn
[PRL135-222504 \(2025\)](#)

Lattice EFT: A many-body EFT solver

- Get *interacting g. s.* from imaginary time projection:

$$|\Psi_{g.s.}\rangle \propto \lim_{\tau \rightarrow \infty} \exp(-\tau H) |\Psi_A\rangle$$

with $|\Psi_A\rangle$ representing A free nucleons.

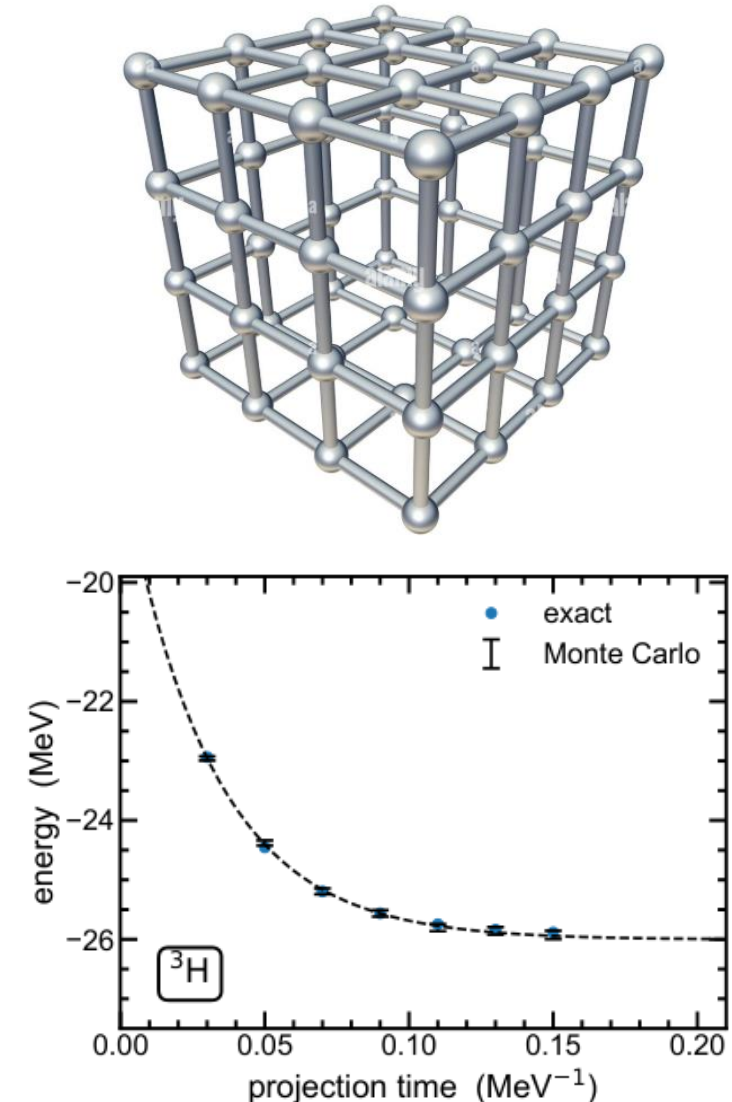
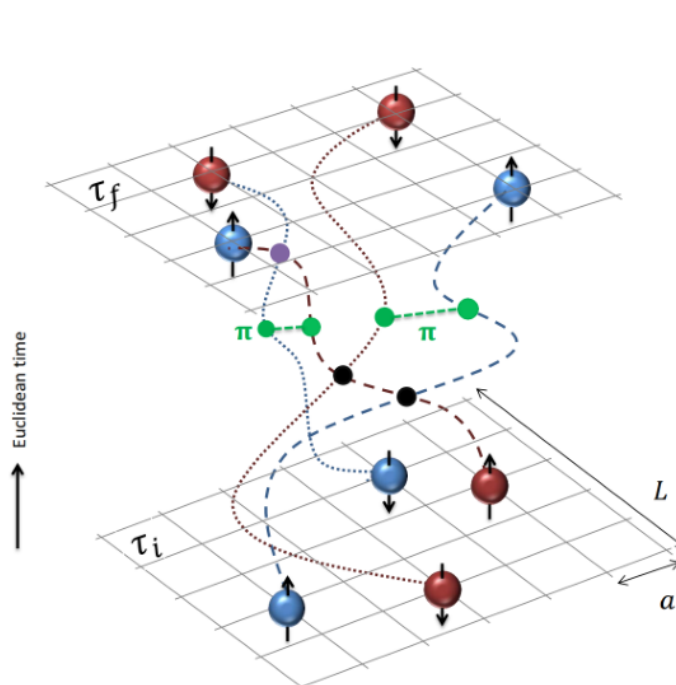
- Expectation value of any operator \mathcal{O} :

$$\langle \mathcal{O} \rangle = \lim_{\tau \rightarrow \infty} \frac{\langle \Psi_A | \exp(-\tau H/2) \mathcal{O} \exp(-\tau H/2) | \Psi_A \rangle}{\langle \Psi_A | \exp(-\tau H) | \Psi_A \rangle}$$

- τ is discretized into time slices:

$$\exp(-\tau H) \simeq \left[: \exp\left(-\frac{\tau}{L_t} H\right) : \right]^{L_t}$$

All possible configurations in $\tau \in [\tau_i, \tau_f]$ are sampled.
Complex structures like nucleon clustering emerges naturally.

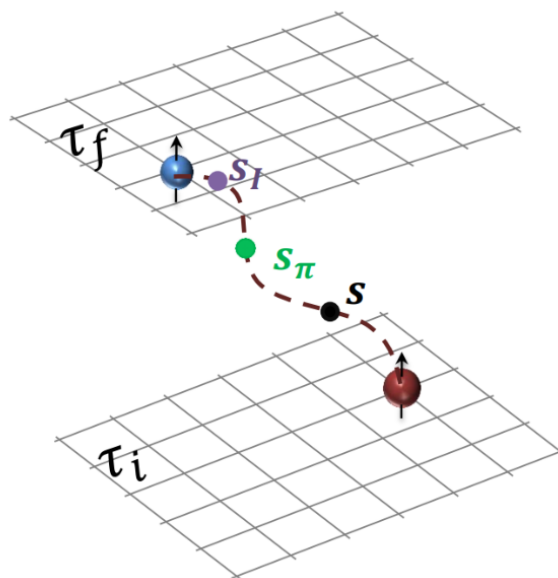
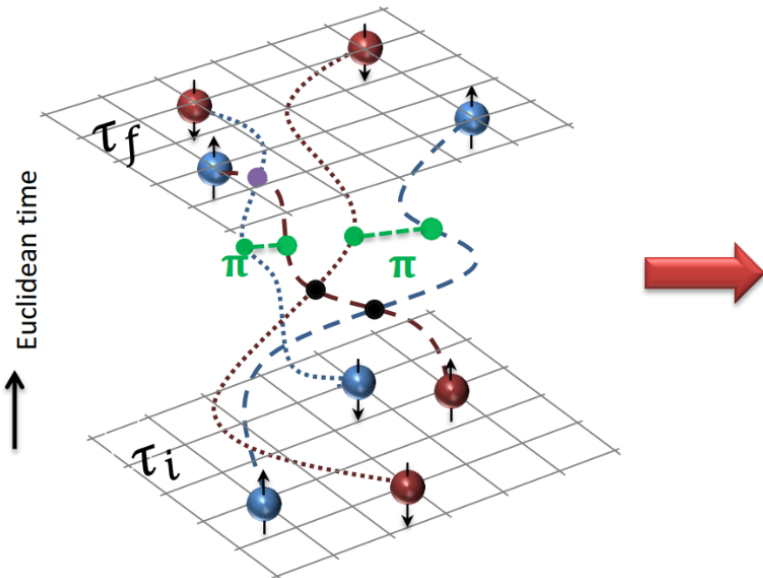


Lattice EFT: A many-body EFT solver

- Quantum correlations between nucleons are represented by fluctuations of the auxiliary fields.

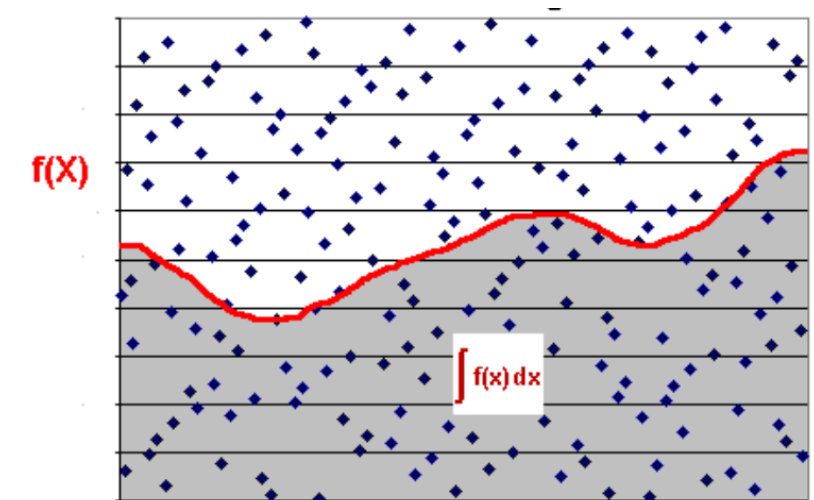
$$: \exp \left[-\frac{a_t C}{2} (\psi^\dagger \psi)^2 \right] := \frac{1}{\sqrt{2\pi}} \int ds : \exp \left[-\frac{s^2}{2} + \sqrt{-a_t C} s (\psi^\dagger \psi) \right] :$$

- Long-range interactions such as OPEP or more complex interactions can be represented similarly.
- For fixed aux. fields, product of s.p. states (e.g., Slater determinant) keep the form of product of s.p. states in propagations. \Leftarrow **No N-N interaction**



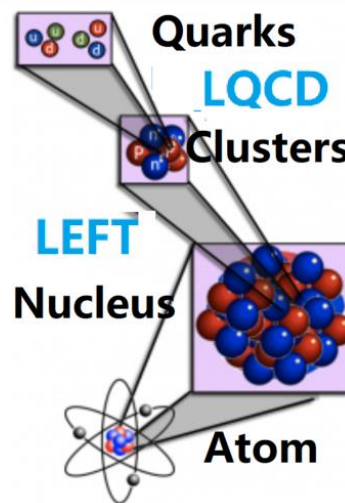
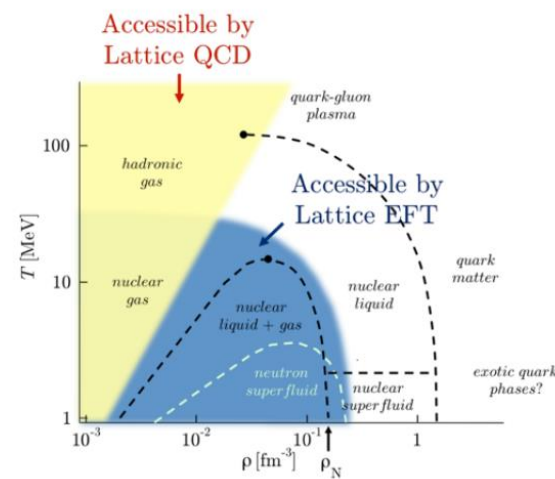
In lattice EFT, solving a general Hamiltonian consists of 5 steps:

1. Rewrite expectation value as a path integral using auxiliary field transformation.
2. For each field configuration, calculate the amplitude.
3. Integrate over the field variables using Monte Carlo algorithms.
4. Take the limit $\tau \rightarrow \infty$ to find the true ground state.
5. Take the limit $L \rightarrow \infty$ to eliminate the finite volume effects.

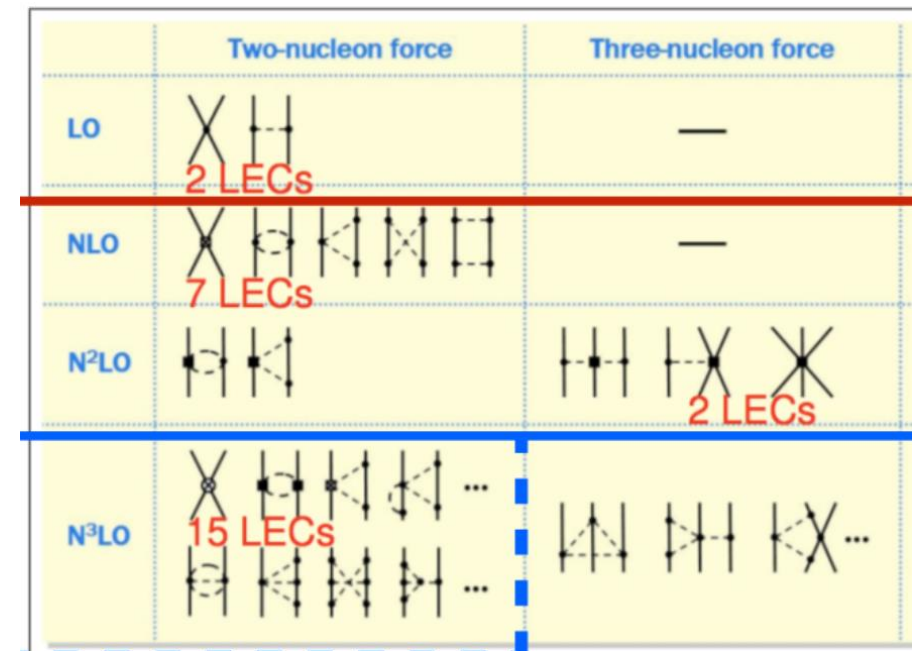


Compare Lattice EFT and Lattice QCD

	LQCD	LEFT
degree of freedom	quarks & gluons	nucleons and pions
lattice spacing	~ 0.1 fm	~ 1 fm
dispersion relation	relativistic	non-relativistic
renormalizability	renormalizable	effective field theory
continuum limit	yes	no
Coulomb	difficult	easy
accessibility	high T / low ρ	low T / ρ_{sat}
sign problem	severe for $\mu > 0$	moderate



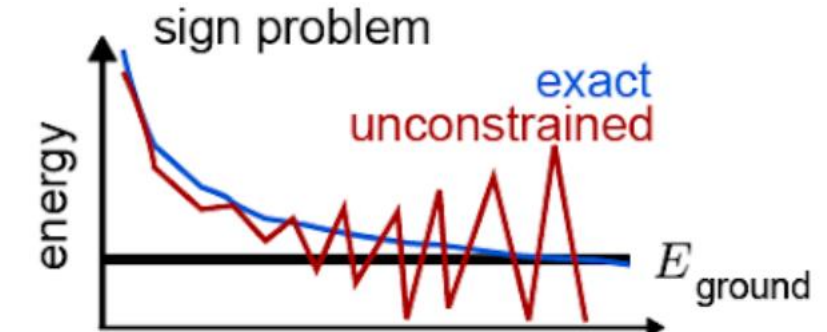
- Lattice EFT share a lot of common features with Lattice QCD. However,
 - Non-rel. \rightarrow particle number conservation
 - Quadratic dispersion relation \rightarrow no Fermion doubling problem
 - EFT contains non-renormalizable terms \rightarrow no continuum limit



Sign problem in quantum Monte Carlo

- **Quantum Monte Carlo** approaches transform the **quantum many-body problems** into high-dimensional integrals that can be evaluated stochastically
- Statistical error $\sim O(N^{-1/2})$
- **Sign problem** occurs when the integrand is NOT positive definite \leftarrow can not be viewed as a **probability distribution**
- Sign problem is severe for **fermionic systems** due to the anti-symmetrization nature of the fermion wave functions
- **Sign-problem-free QMC** exists but confined to toy-models \leftarrow can be solved with exactly polynomial complexity
 1. Sign problem might be tolerable for light nuclei. **However**, any sign problem increases exponentially with the particle number \leftarrow **exponential complexity returns!**
 2. Sign problem might be partially solved by constrained path / perturbation theory. **However**, these require systematic expansion and induces **systematic biases**.

Sign-problem-free QMC allows us to solve the nuclear many-body problem from light to heavy nuclei with remarkably high numerical precision.
Yet its potential has not been fully exploited.



Examples of sign-problem-free QMC

- **Lattice QCD** with two identical quark species

$$Z = \int \mathcal{D}\psi \mathcal{D}\bar{\psi} \mathcal{D}[U] e^{-S_G[U]} \det[D[U]], \quad \det[D[U]] = \det[D_u[U]] \det[D_d[U]] = \det[D_u[U]]^2 > 0$$

- **Nuclear Lattice EFT** with Wigner-SU(4) interactions (even-even nuclei)

$$Z = \int \mathcal{D}s e^{-s^2/2} \det[Z(s)], \quad \det[Z(s)] = \det[Z_\uparrow(s)] \det[Z_\downarrow(s)] = \det[Z_\uparrow(s)]^2 \geq 0$$

- Repulsive Fermi-Hubbard model at half-filling
- Kane-Mele-Hubbard model
- Half-filled Kondo lattice model

Positivity of the fermionic determinant is protected by the time-reversal symmetry

Sufficient condition for absence of the sign problem in the fermionic quantum Monte Carlo algorithm, C.-J. Wu and S.-C. Zhang, PRB71, 155115 (2005)

Sign-problem-free fermionic quantum Monte Carlo: Developments and Applications, Z.-X. Li and H. Yao, Annu. Rev. Condens. Matter Phys. 10, 337 (2019)

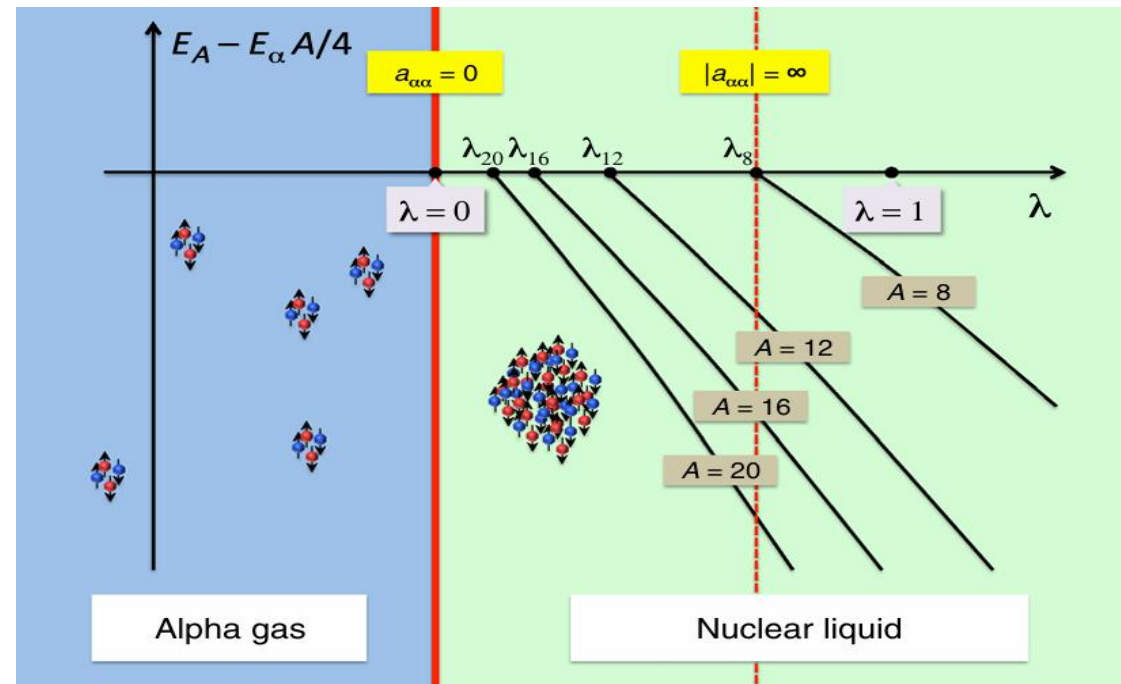
Nuclear binding near a quantum phase transition

$$H_{\text{SU4}} = H_{\text{free}} + \frac{1}{2!} C_2 \sum_{\mathbf{n}} \bar{\rho}(\mathbf{n})^2$$

$$\bar{\rho}(\mathbf{n}) = \rho(\mathbf{n}) + s_L \sum_{|\mathbf{n}' - \mathbf{n}|=1} \rho(\mathbf{n}')$$

$$\rho(\mathbf{n}) = \overline{\Psi}^\dagger(\mathbf{n})\overline{\Psi}(\mathbf{n})$$

$$\bar{\Psi}(\mathbf{n}) = \Psi(\mathbf{n}) + s_{\text{NL}} \sum_{|\mathbf{n}' - \mathbf{n}|=1} \Psi(\mathbf{n}')$$



Challenge: Minimal nuclear force
That reproduce the binding pattern

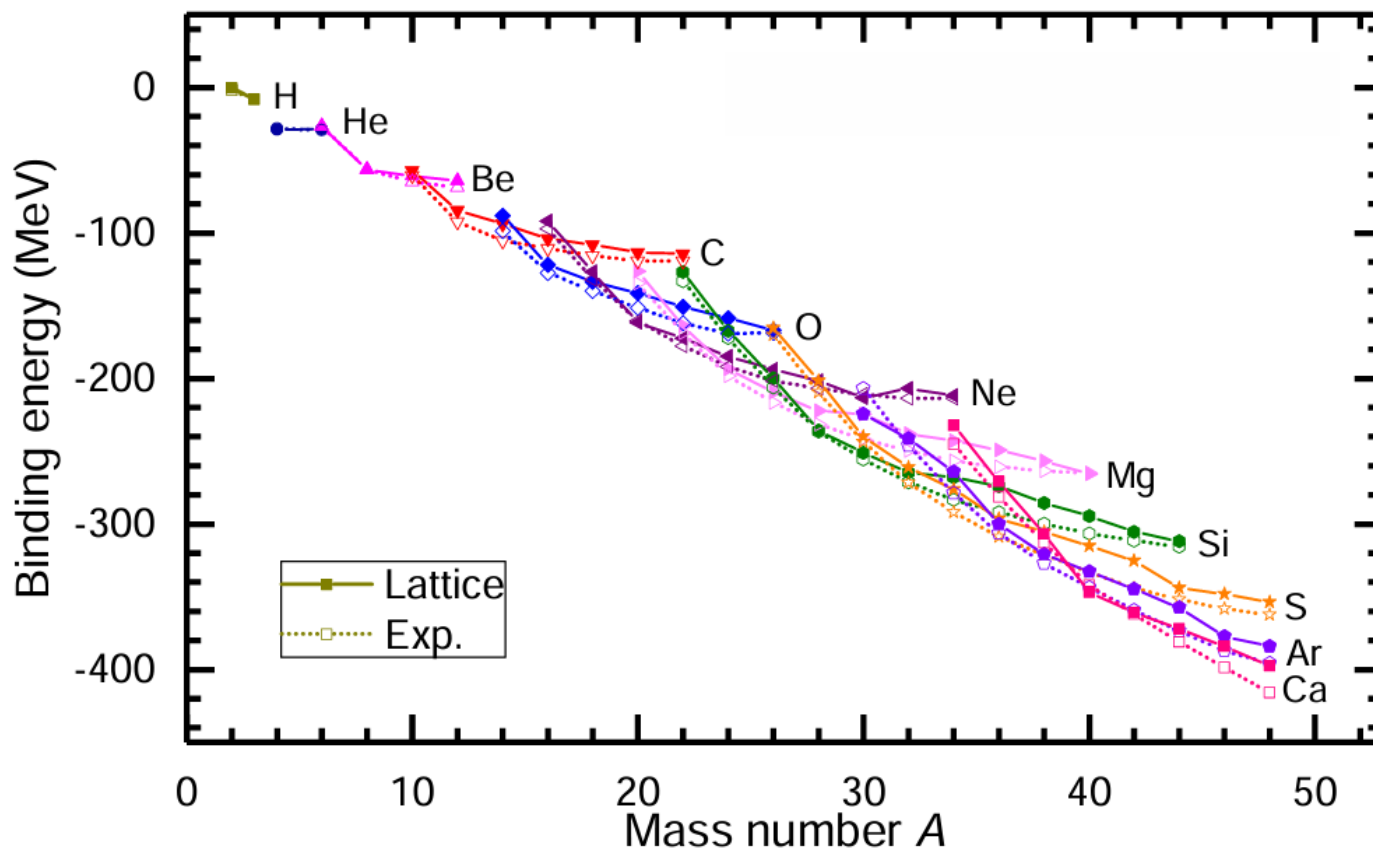
Simple Wigner-SU(4) central force fails!

- The nuclear force can be either local (position-dependent) or non-local (velocity-dependent).
- Locality is an essential element for nuclear binding.

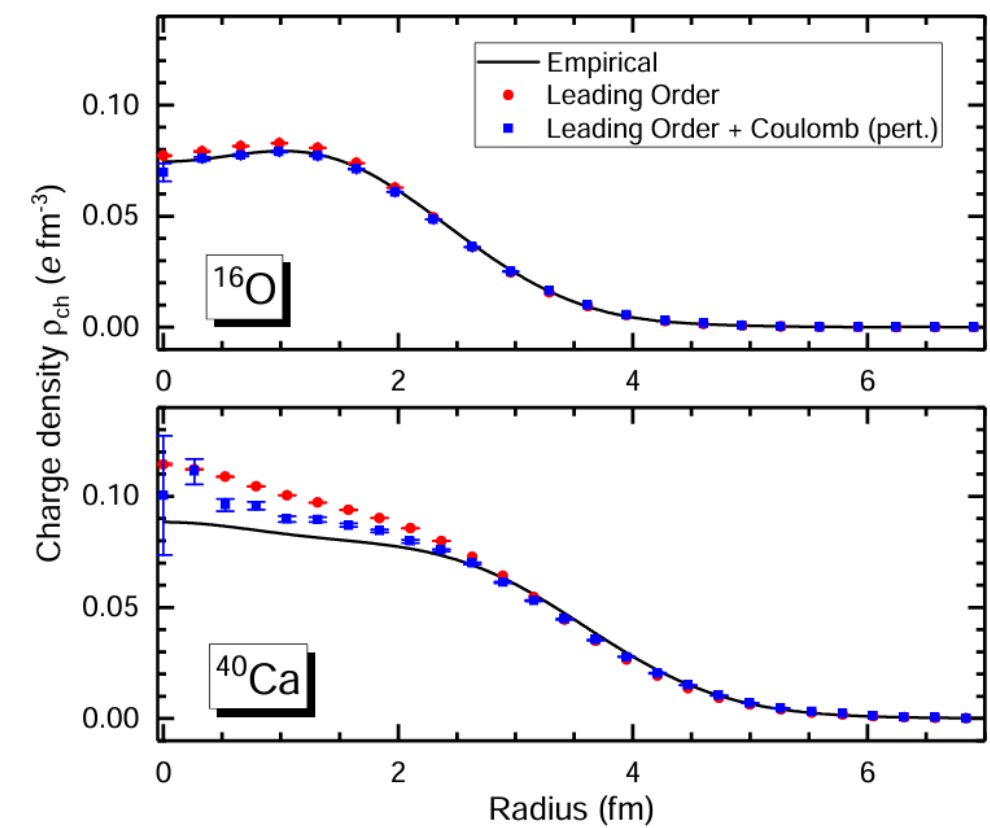
S. Elhatisari et al., PRL 117, 132051 (2016)

Nuclear force with a Wigner-SU(4) symmetry

$$H_{\text{SU}(4)} = H_{\text{free}} + \frac{1}{2!} C_2 \sum_{\mathbf{n}} \tilde{\rho}(\mathbf{n})^2 + \frac{1}{3!} C_3 \sum_{\mathbf{n}} \tilde{\rho}(\mathbf{n})^3$$

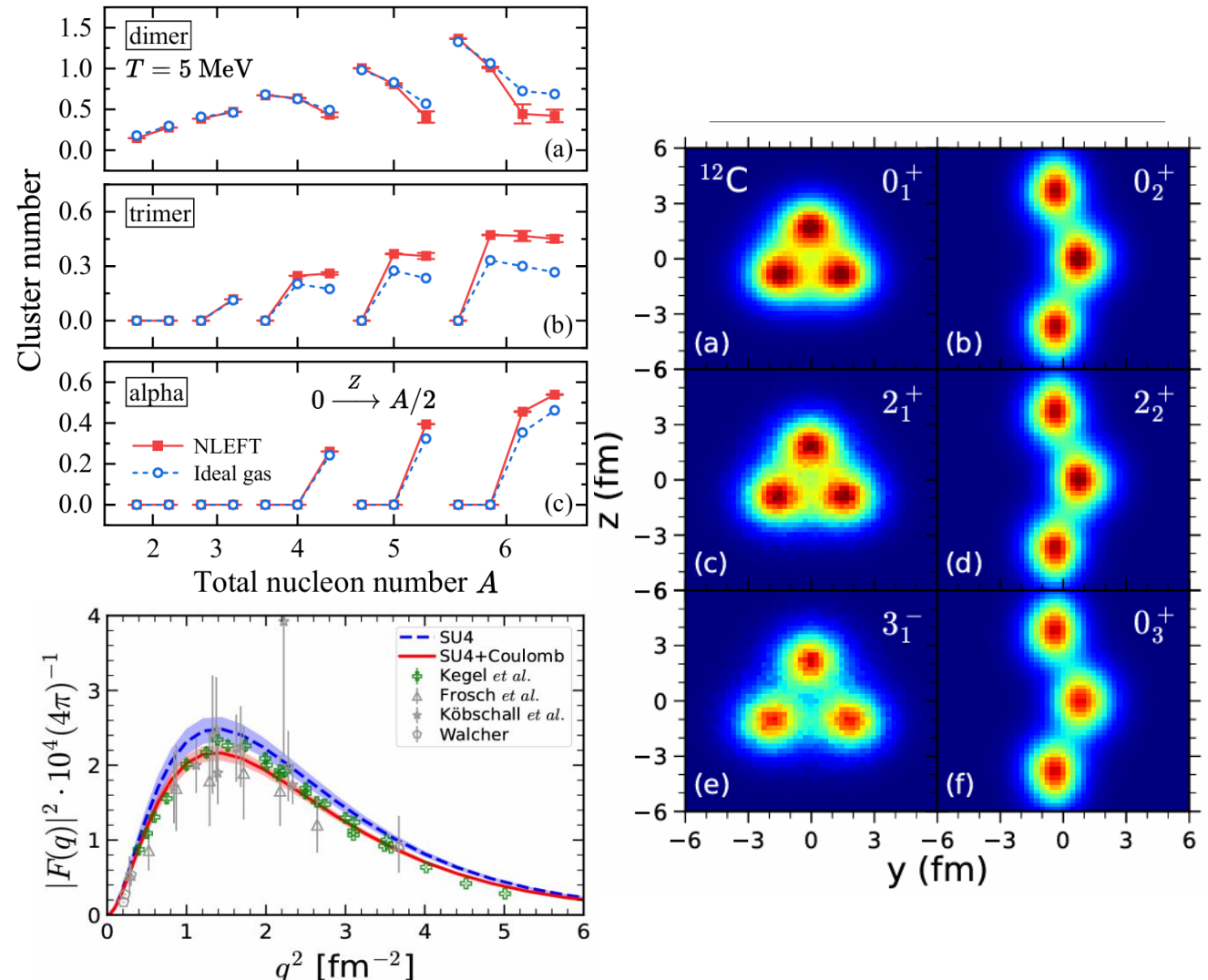


All density operators are smeared
Lu et al., PLB 797, 134863 (2019)



Applications of Wigner-SU(4) interaction

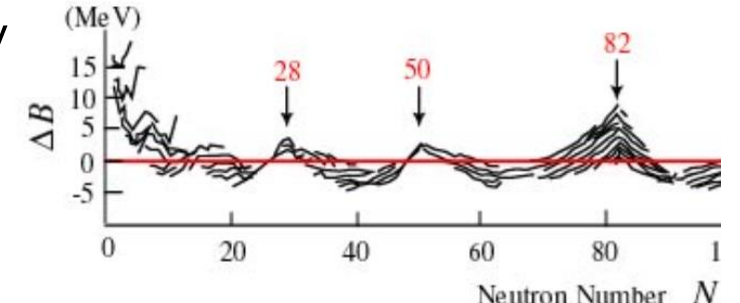
- Ab initio calculations of the isotopic dependence of nuclear clustering, [S. Elhatisari et al., PRL 119, 222505 \(2017\)](#)
- Emergent geometry and duality in the carbon nucleus, [S. Shen et al., EPJA 57, 276 \(2021\)](#); [S. Shen et al., Nat. Comm. 14, 2777 \(2023\)](#);
- Ab initio study of nuclear clustering in hot dilute nuclear matter, [Z. Ren et al., PLB 850, 138463 \(2024\)](#)
- Ab initio calculation of the alpha-particle Monopole transition form factor, [Ulf-G. Meißner et al., PRL 132, 062501 \(2024\)](#)
- Ab initio study of the beryllium isotopes ^7Be to ^{12}Be , [S. Shen et al., PRL 134, 162503 \(2025\)](#)
-



Improved Wigner-SU(4) interaction

- **Wigner-SU(4) symmetry** is an approximate symmetry
-Lack correct **shell structure** \rightarrow Spin-orbit coupling
- We introduce a **spin-orbit coupling**

$$H = \sum_n \left[-\frac{\Psi^\dagger \nabla^2 \Psi}{2M} + \frac{C_2}{2} \bar{\rho}^2 + \frac{C_3}{6} \bar{\rho}^3 + C_s \bar{\rho} \bar{\rho}_s \right] \quad \rho = \bar{a}^\dagger \bar{a}, \quad \rho_s = \sum_{ijk} \epsilon_{ijk} \nabla_i \left[\bar{a}^\dagger (\vec{\nabla}_j - \vec{\nabla}_j) \sigma_k \bar{a} \right]$$



- **Wigner-SU(4) symmetry** does not mix **spin-up** and **spin-down** particles
 \rightarrow Fermion determinant factorized into **two identical parts**: $\det(Z) = \det(Z_\uparrow)^2 \geq 0$
 \rightarrow Fermionic **sign problem avoided!**
- **Spin-orbit term** act equivalently for **spin-up** and **spin-down** particles
 \rightarrow Fermion determinant keeps positive definite

Proof for the positivity of the determinant

$$\begin{aligned}\langle O \rangle &= \lim_{\tau \rightarrow \infty} \frac{\langle \Phi_T | e^{-\tau H/2} O e^{-\tau H/2} | \Phi_T \rangle}{\langle \Phi_T | e^{-\tau H} | \Phi_T \rangle} = \lim_{L_t \rightarrow \infty} \frac{\langle \Phi_T | M^{L_t/2} O M^{L_t/2} | \Phi_T \rangle}{\langle \Phi_T | M^{L_t} | \Phi_T \rangle} \\ &= \lim_{L_t \rightarrow \infty} \frac{\int \mathcal{D}c \exp(-\sum_{i=1}^{L_t} c_i^2/2) \langle \Phi_T | M(c_{L_t}) \cdots M(c_{L_t/2+1}) O M(c_{L_t/2}) \cdots M(c_1) | \Phi_T \rangle}{\int \mathcal{D}c \exp(-\sum_{i=1}^{L_t} c_i^2/2) \langle \Phi_T | M(c_{L_t}) \cdots M(c_1) | \Phi_T \rangle}\end{aligned}$$

$$M(c) = \exp \left[\sum_{\mathbf{n}, \mathbf{n}'} a_t \frac{\Psi^\dagger(\mathbf{n}) \nabla_{\mathbf{n}\mathbf{n}'}^2 \Psi(\mathbf{n}')}{2M} + \sum_{\mathbf{n}} \sqrt{-a_t C_2} c(\mathbf{n}) \left(\bar{\rho}(\mathbf{n}) + \frac{C_s}{2C_2} \bar{\rho}_s(\mathbf{n}) \right) \right]$$

$$Z(c) = [\langle \phi_i | \bar{M}(c) | \phi_j \rangle]_{i,j=1}^A = \begin{pmatrix} \langle \phi_1 | \bar{M}(c) | \phi_1 \rangle & \langle \phi_1 | \bar{M}(c) | \phi_2 \rangle & \cdots & \langle \phi_1 | \bar{M}(c) | \phi_A \rangle \\ \langle \phi_2 | \bar{M}(c) | \phi_1 \rangle & \langle \phi_2 | \bar{M}(c) | \phi_2 \rangle & \cdots & \langle \phi_2 | \bar{M}(c) | \phi_A \rangle \\ \vdots & \vdots & \ddots & \vdots \\ \langle \phi_A | \bar{M}(c) | \phi_1 \rangle & \langle \phi_A | \bar{M}(c) | \phi_2 \rangle & \cdots & \langle \phi_A | \bar{M}(c) | \phi_A \rangle \end{pmatrix}$$

For even-even nuclei, we prepare the single nucleon wave functions as paired by the time-reversal operation:

$$|\phi_{A/2+k}\rangle = \mathcal{T}|\phi_k\rangle, \quad k = 1, 2, \dots, A/2, \quad (22)$$

where $\mathcal{T} = i\sigma_y \mathcal{K}$ is the time-reversal operator and \mathcal{K} denotes complex conjugation. The matrix $\bar{M}(c)$ commutes with \mathcal{T} . Using the properties of \mathcal{T} and Eq. (22), we obtain the relations:

$$\begin{aligned}\langle \phi_{A/2+i} | \bar{M}(c) | \phi_{A/2+j} \rangle &= \langle \mathcal{T}\phi_i | \bar{M}(c) | \mathcal{T}\phi_j \rangle = \langle \phi_i | \bar{M}(c) | \mathcal{T}^\dagger \mathcal{T}\phi_j \rangle^* = \langle \phi_i | \bar{M}(c) | \phi_j \rangle^*, \\ \langle \phi_{A/2+i} | \bar{M}(c) | \phi_j \rangle &= \langle \mathcal{T}\phi_i | \bar{M}(c) | \phi_j \rangle = \langle \phi_i | \bar{M}(c) | \mathcal{T}^\dagger \phi_j \rangle^* = -\langle \phi_i | \bar{M}(c) | \phi_{A/2+j} \rangle^*\end{aligned}$$

- The nucleons evolve **independently** under the auxiliary fields.
- Time-reversal pairs are **NOT** broken by the **spin-orbit coupling**
- Matrix elements of the fermionic correlation matrix respect a **special symmetry**

Proof for the positivity of the determinant

The correlation matrix then has the structure:

$$Z = \begin{pmatrix} U & -V^* \\ V & U^* \end{pmatrix}, \quad (24)$$

where U and V are $A/2 \times A/2$ complex matrices.

We define a spin-flipping matrix:

$$\Sigma = i\sigma_y \otimes I_{A/2} = \begin{pmatrix} 0 & I_{A/2} \\ -I_{A/2} & 0 \end{pmatrix}, \quad (25)$$

where $I_{A/2}$ is the $A/2 \times A/2$ identity matrix. Direct verification shows that

$$Z\Sigma = \Sigma Z^*. \quad (26)$$

For any eigenvalue $\lambda \in \mathbb{C}$ with corresponding eigenvector v satisfying $Zv = \lambda v$, we have

$$Z(\Sigma v^*) = \Sigma Z^* v^* = \Sigma(\lambda^* v^*) = \lambda^* (\Sigma v^*), \quad (27)$$

implying that λ^* is also an eigenvalue with eigenvector $w = \Sigma v^*$. Thus, complex eigenvalues of Z always appear in conjugate pairs. If λ is real, we find

$$\langle v | w \rangle = v^\dagger \Sigma v^* = (v^T \Sigma v)^* = 0, \quad (28)$$

indicating that v and w are orthogonal eigenvectors corresponding to the same real eigenvalue. In this case, the real eigenvalue appears twice in the diagonalized form of Z . Consequently, the determinant $\det(Z)$, being the product of all eigenvalues, is always nonnegative.

Gradient Descent method

- We fit to binding energies of ^4He , ^{16}O , ^{24}Mg , ^{28}Si , ^{32}S , ^{40}Ca using a **derivative-based** optimization method

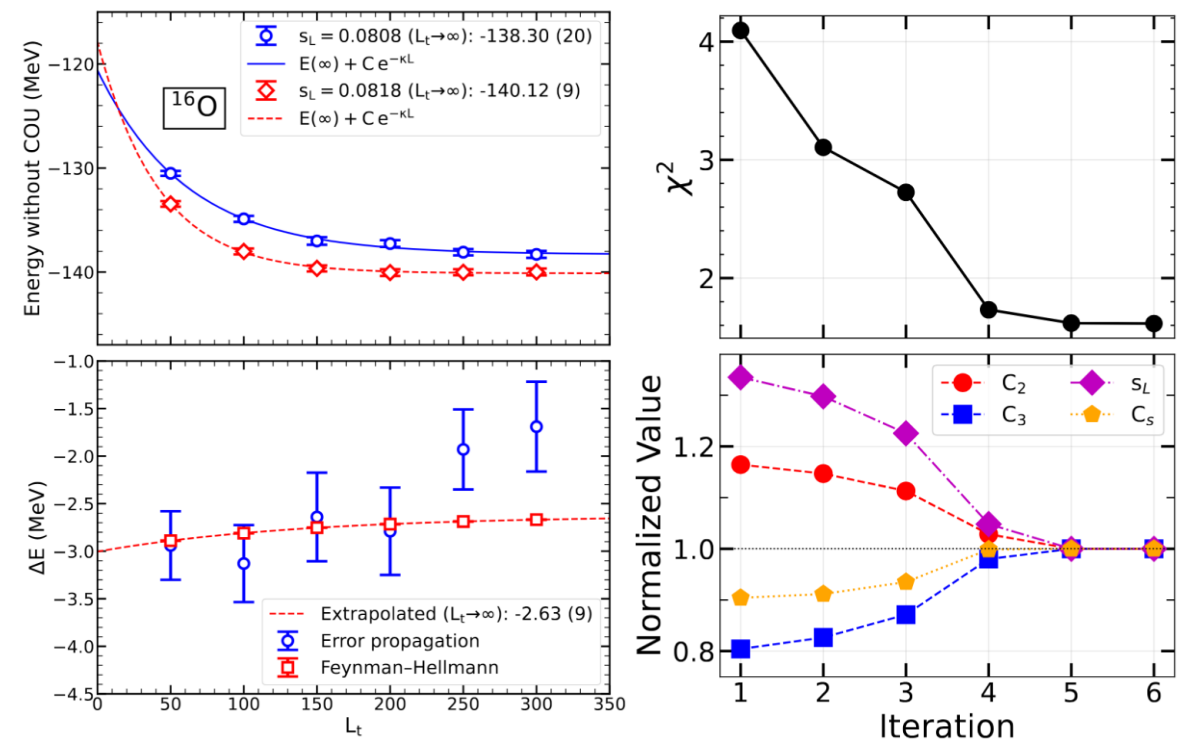
$$\chi^2 = \sum_A \left[\frac{E(A) - E_{\text{exp}}(A)}{\Delta(A)} \right]^2$$

- The derivatives are calculated using the **Feynman-Hellmann theorem**,

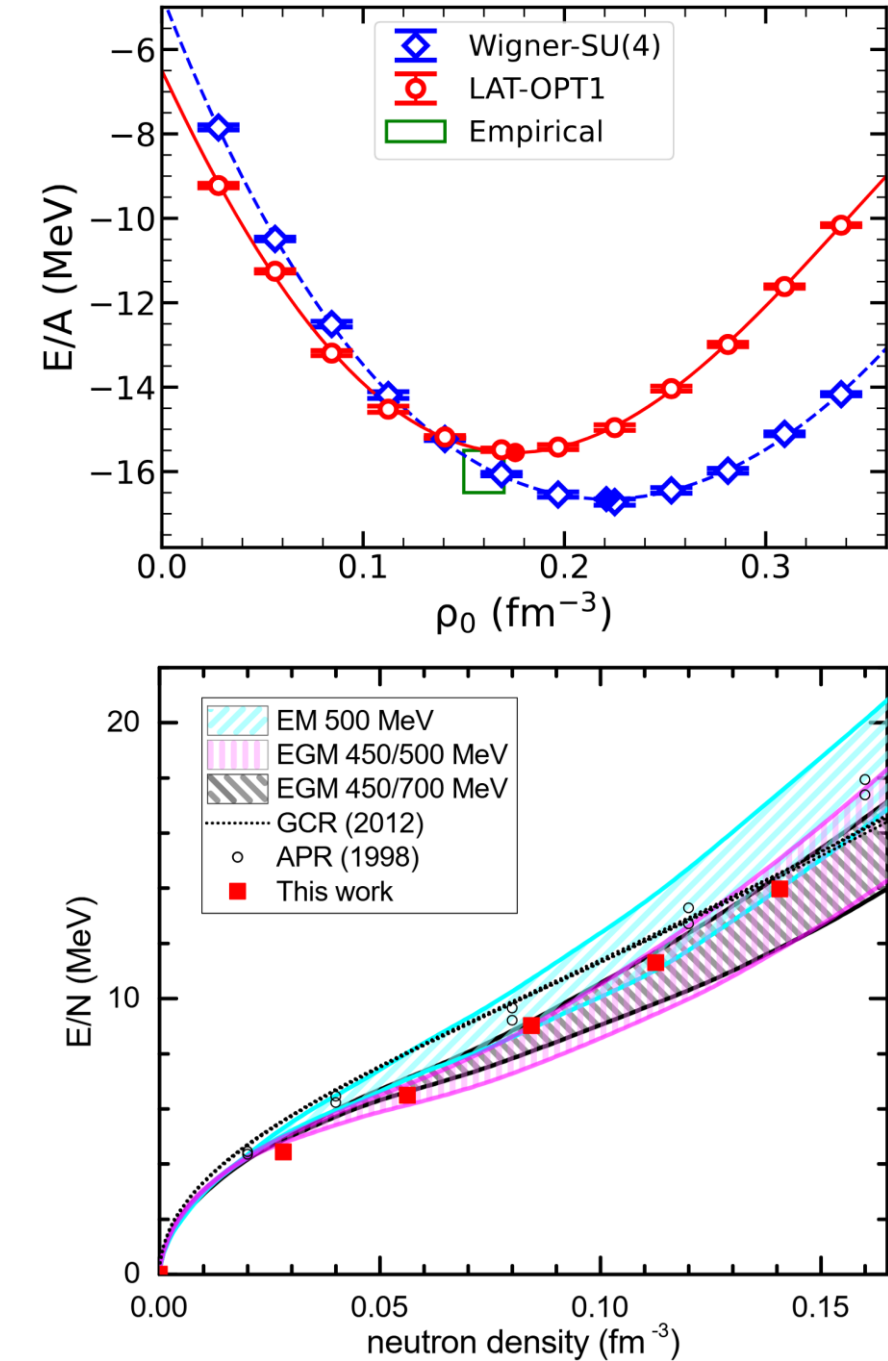
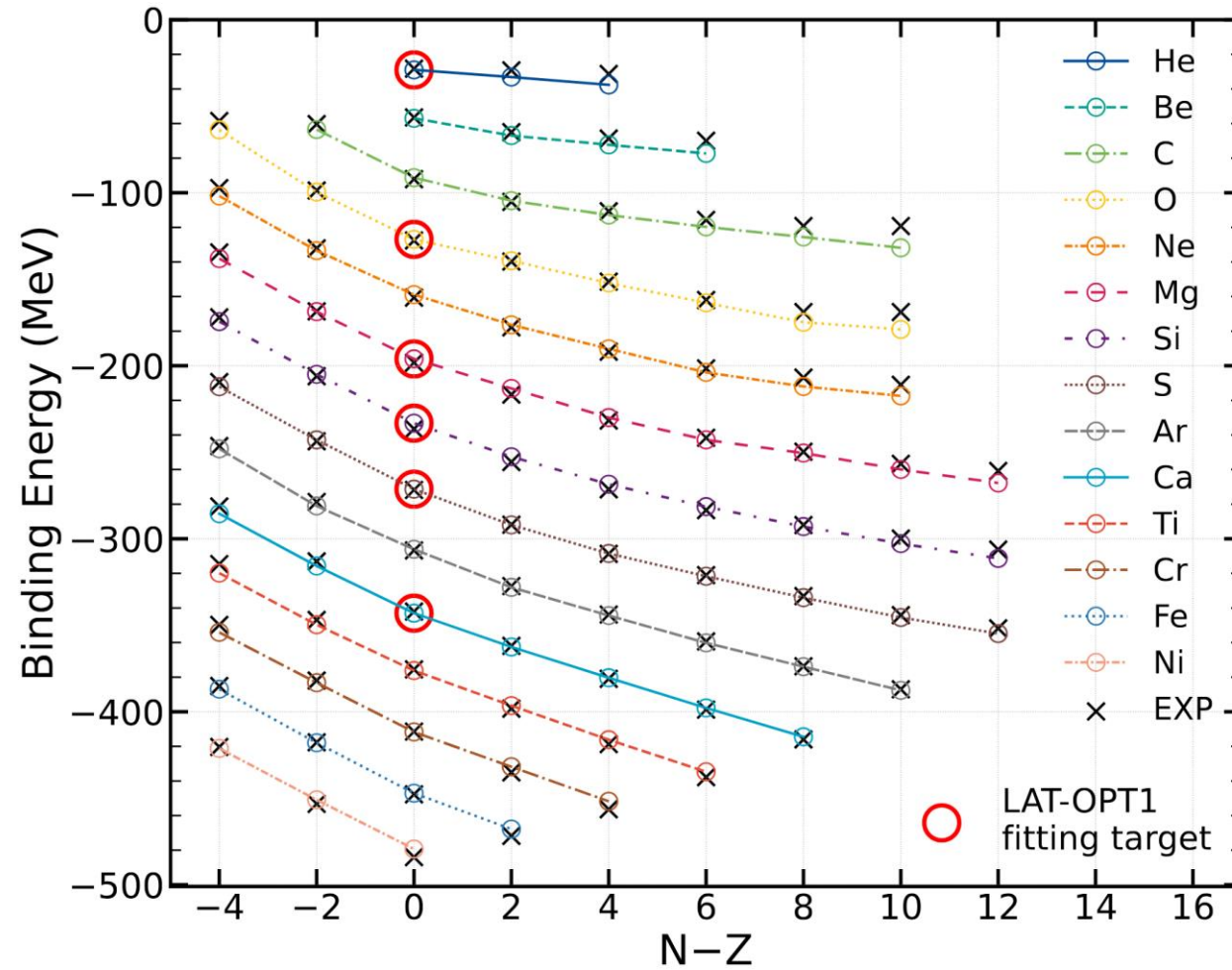
$$\partial E(A)/\partial x = \langle \Phi | H(x + \delta) - H(x) | \Phi \rangle / \delta$$

- Typically converge within 10 iterations
 ← **precise and unbiased**
 derivative computation is essential!

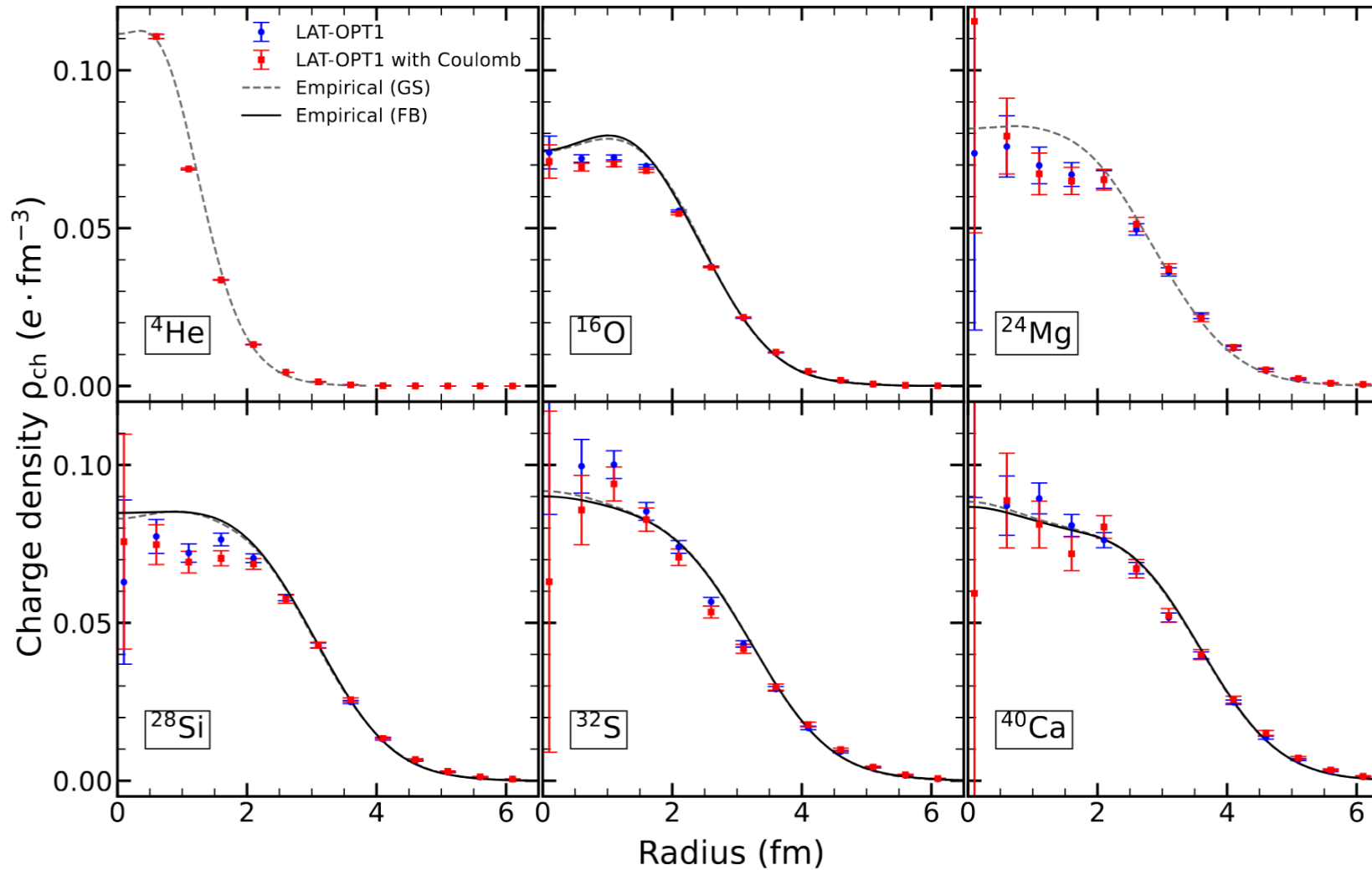
$$C_2 = -4.410 \times 10^{-7} \text{ MeV}^{-2}, C_3 = 1.561 \times 10^{-15} \text{ MeV}^{-5}, C_s = 8.590 \times 10^{-12} \text{ MeV}^{-4}, s_L = 0.081, s_{NL} = 0.45 \quad \text{"LAT-OPT1"}$$



Results from LAT-OPT1



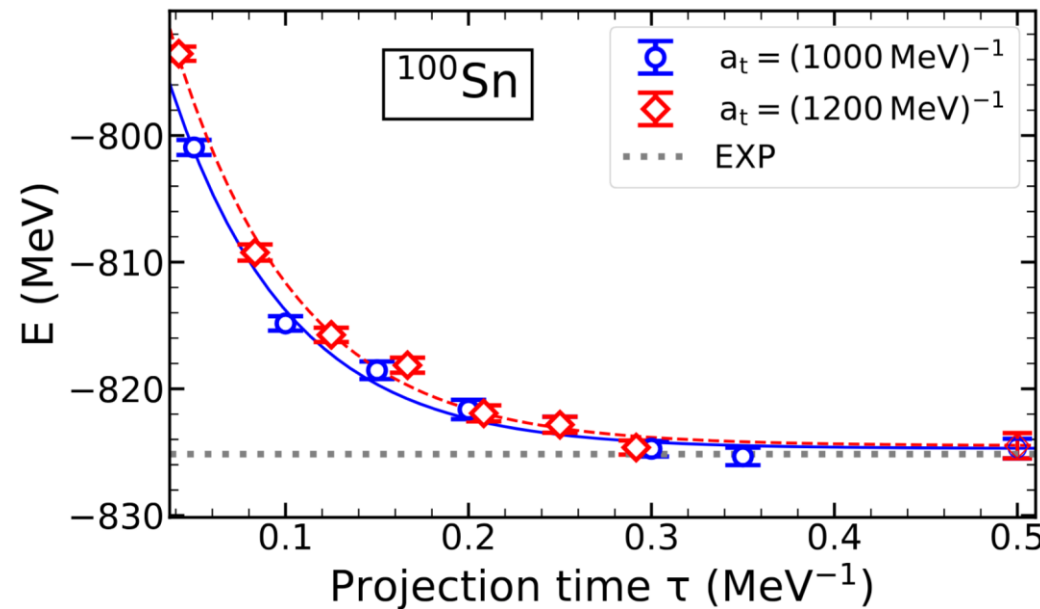
Results from LAT-OPT1: Charge densities



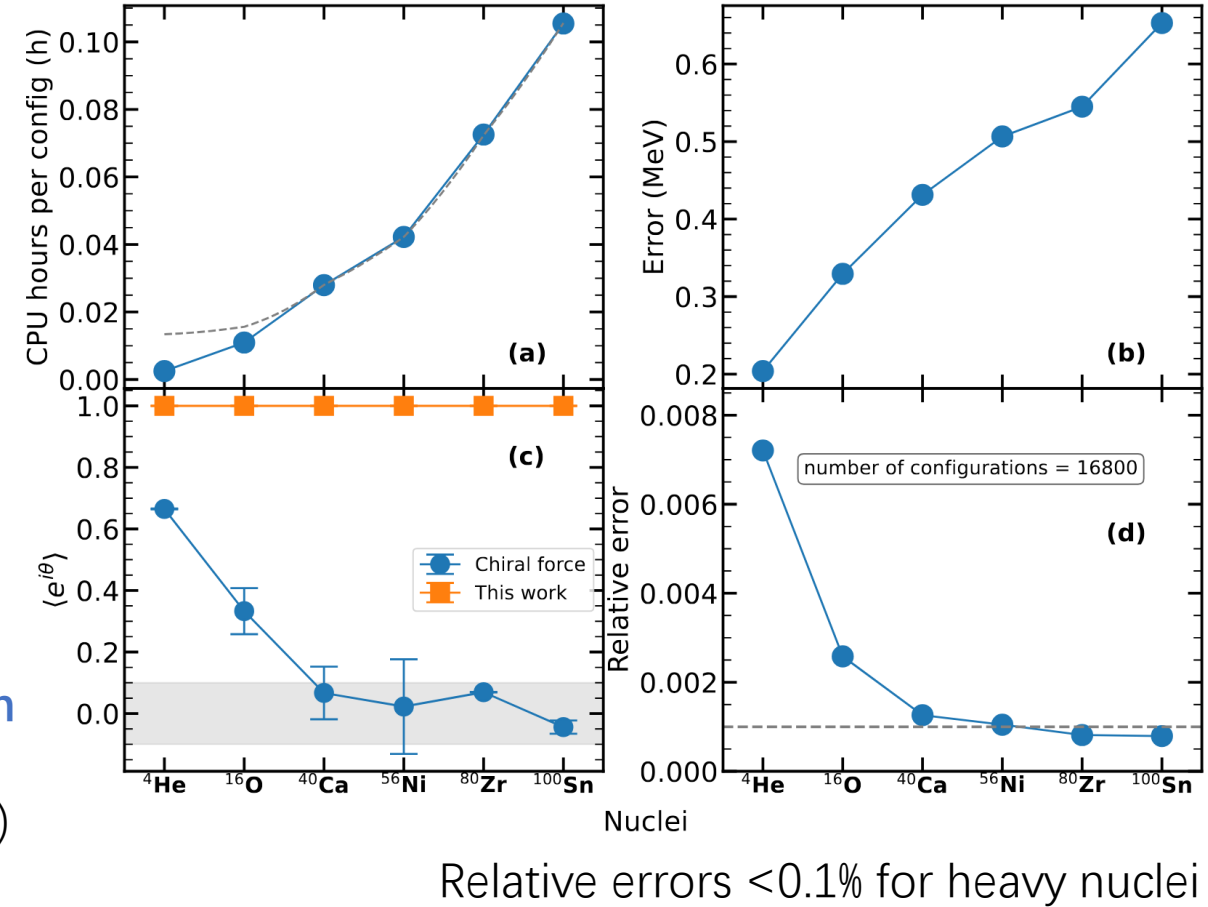
- Charge densities calculated using **pinhole algorithm**
Elhatisari et al., PRL119, 222505 (2017)
- **Pinhole algorithm** induce **mild sign problem**, not available for $A >= 40$.
See **partial pinhole algorithm** for a solution
Zheng-Xue Ren et al., PRL135-152502 (2025)

Results from LAT-OPT1: Heavy nuclei

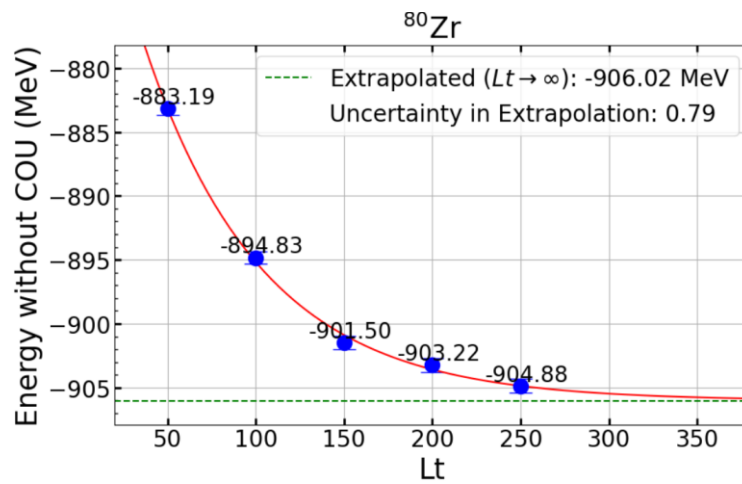
- Sign-problem-free QMC scales polynomially towards heavy nuclei



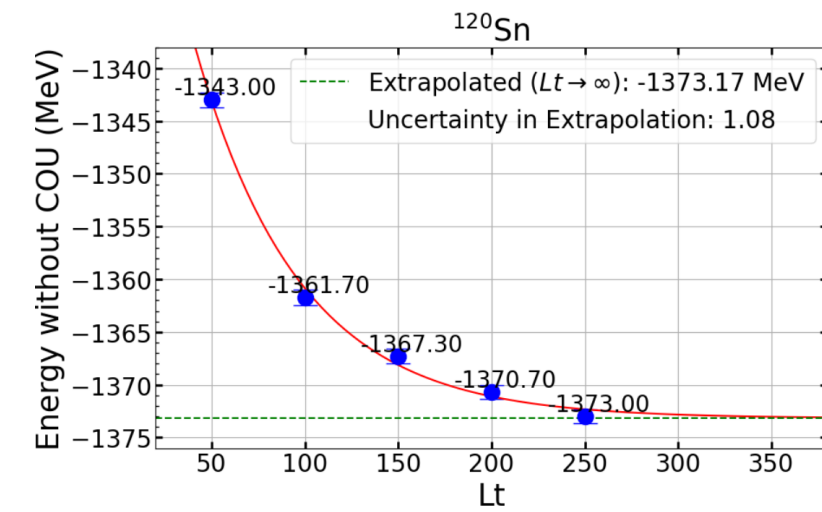
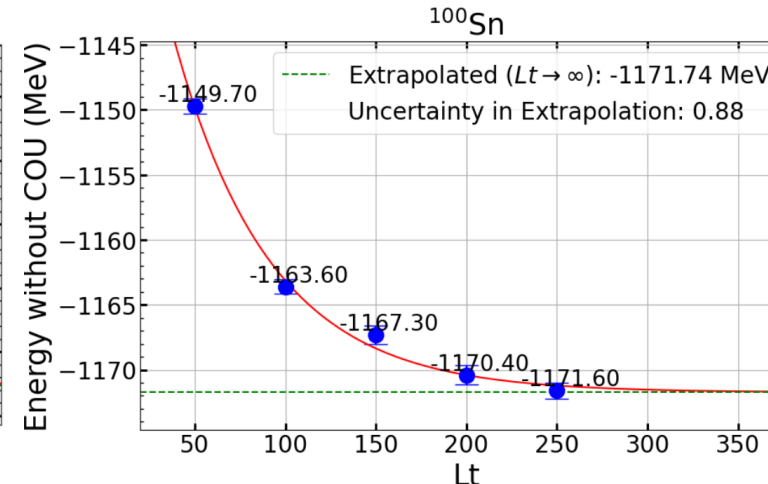
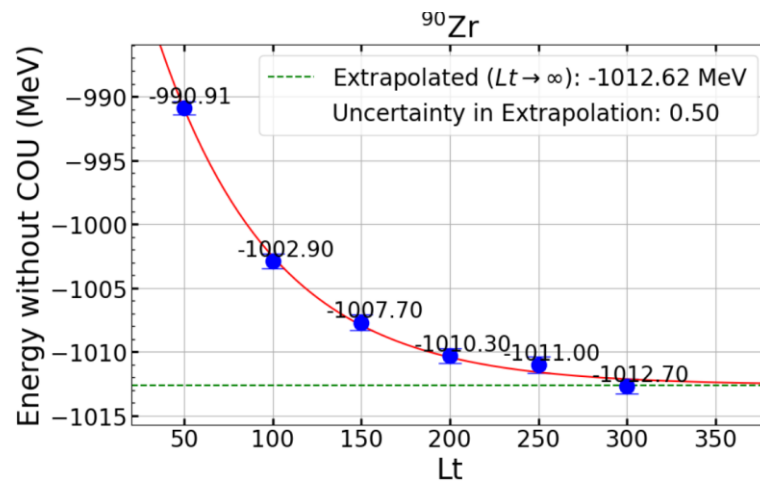
Extract binding energy of ^{100}Sn with **~1 MeV precision**
using **~30000 CPU hours**
(10 days on AMD EPYC [9554@3.1GHz](#), 128 CPU cores)



Results from LAT-OPT1: Heavy nuclei



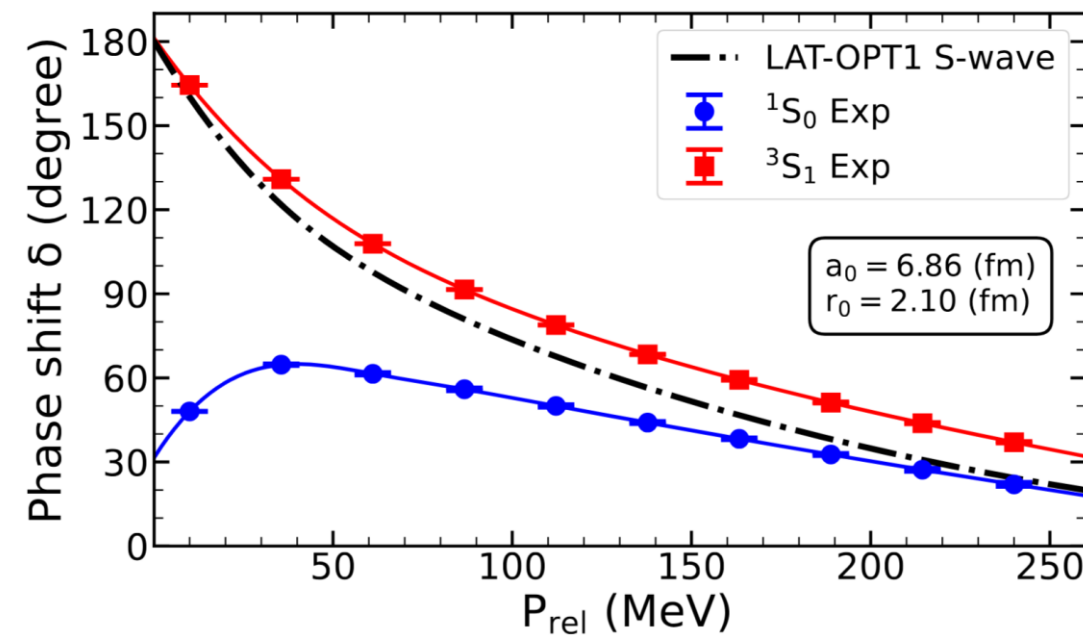
Nucleus	E_{bind} (MeV)	E_{sl} (MeV)	$E_{\text{sl}}/E_{\text{bind}}$	EXP (MeV)
⁴ He	-29.0(2)	-0.3	0.010	-28.3
¹² C	-91.3(1)	-13.3	0.146	-92.2
¹⁴ C	-104.6(1)	-12.7	0.121	-105.3
¹⁶ O	-126.9(2)	-5.6	0.044	-127.6
⁴⁰ Ca	-343.0(2)	-13.6	0.040	-342.1
⁴⁸ Ca	-414.5(3)	-42.3	0.102	-416.0
⁵⁶ Ni	-479.3(6)	-74.6	0.156	-484.0
⁸⁰ Zr	-672.1(8)	-23.3	0.035	-669.2
⁹⁰ Zr	-782.1(5)	-64.8	0.083	-783.9
¹⁰⁰ Sn	-824.7(8)	-103.0	0.125	-825.2
¹³² Sn	-1134.2(27)	-110.9	0.098	-1102.8



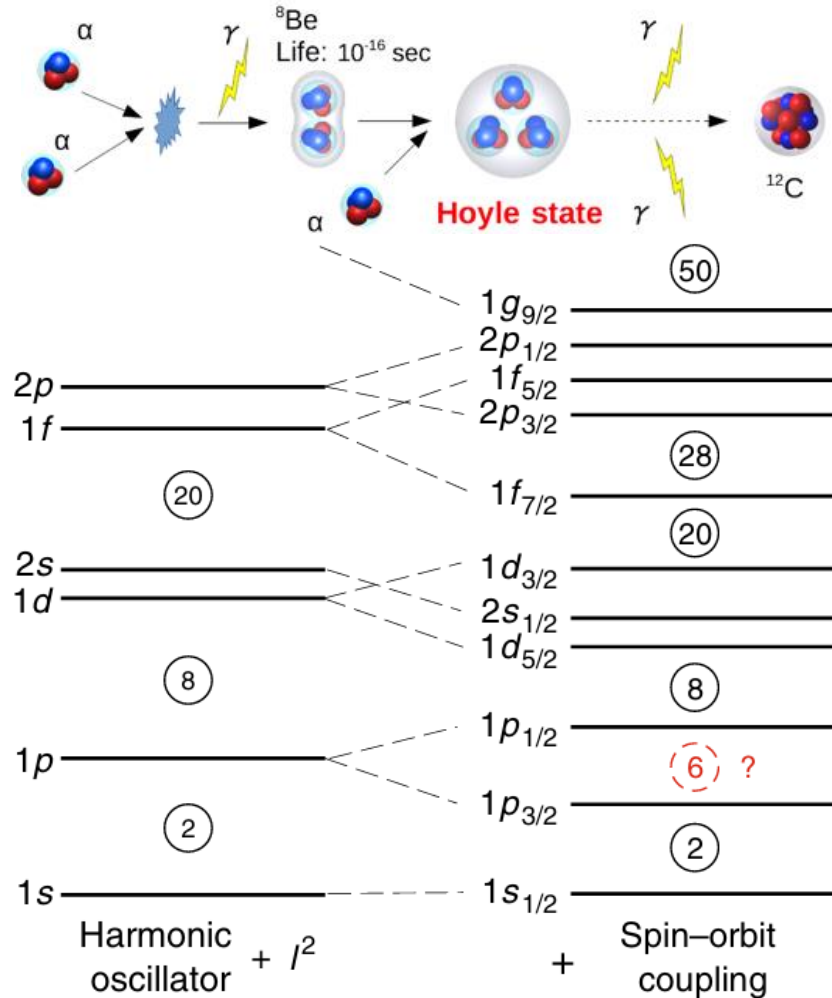
- Spin-orbit energy enhanced for **new magic numbers** 28, 50, 82, etc., indicating **shell structure emergence**
- Remarkable **generalization capability** ← all **quantum correlation** included

Results from LAT-OPT1: Phase shifts

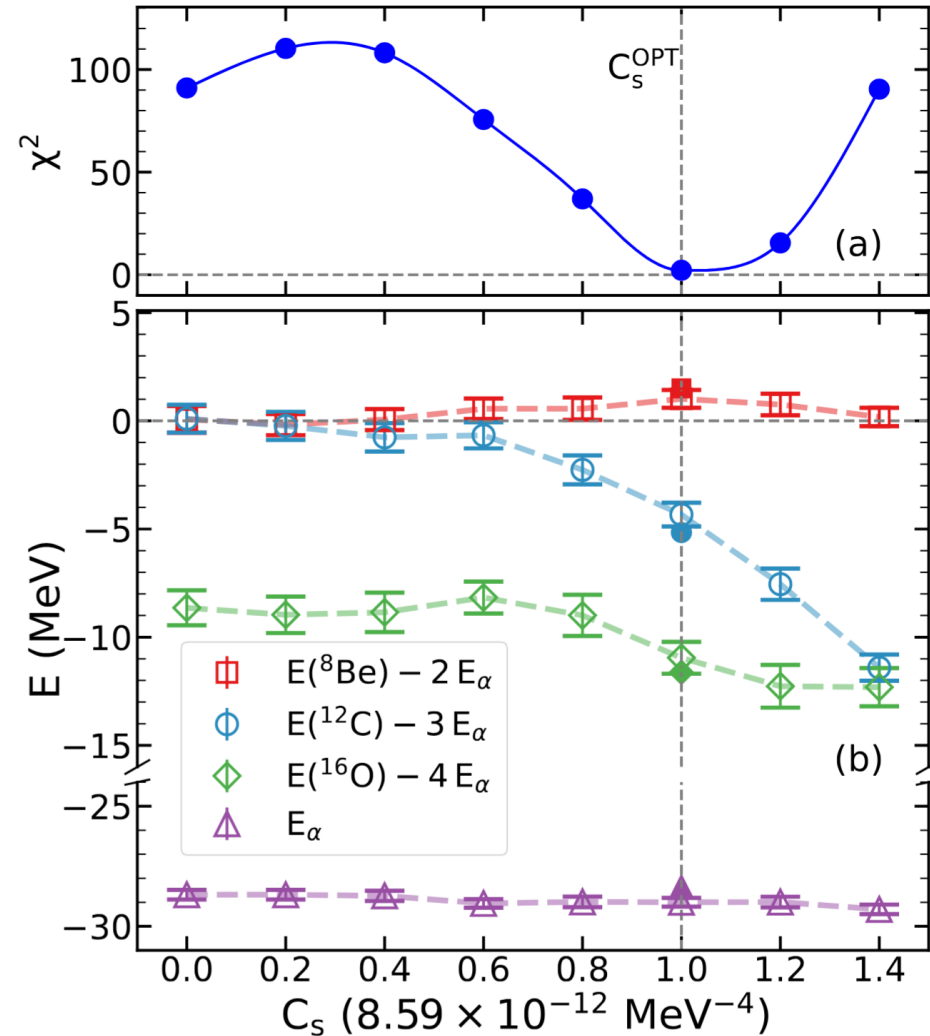
- *Ab initio calculations* attempt to predict **finite nuclei** from **phase shifts**
- Conversely, we can also predict **phase shifts** from **finite nuclei**
 - ← Binding energies and charge radii can be measured with **extremely high precision**, encoding **complete** information about nuclear forces.
- The nuclear force fitted to **binding energies** predict a **S-wave phase shift** falling between $1S_0$ and $3S_1$
- S-wave splitting, S-D mixing, P-wave phase shifts should be reproduced at **higher orders**



Results from LAT-OPT1: Nuclear clustering



D. T. Tran et al., Nat. Comm. 9, 1594 (2018)



Exactly solvable phenomenological nuclear force

- *Ab initio* calculations

- Realistic interactions fitted to few-body data
- Challenging to solve, particularly for heavy nuclei

$$V(1, 2) = t_0(1 + x_0 P^\sigma) \delta(\mathbf{r}_1 - \mathbf{r}_2) + \frac{1}{2} t_1 [\delta(\mathbf{r}_1 - \mathbf{r}_2) \mathbf{k}^2 + \mathbf{k}^2 \delta(\mathbf{r}_1 - \mathbf{r}_2)] + t_2 \mathbf{k} \delta(\mathbf{r}_1 - \mathbf{r}_2) \mathbf{k} + i W_0 (\sigma^{(1)} + \sigma^{(2)}) \mathbf{k} \times \delta(\mathbf{r}_1 - \mathbf{r}_2) \mathbf{k},$$

- Phenomenological methods

- Phenomenological interactions fitted to finite nuclei
- Easy to solve, however lack correlations

$$V(1, 2, 3) = t_3 \delta(\mathbf{r}_1 - \mathbf{r}_2) \delta(\mathbf{r}_2 - \mathbf{r}_3)$$

- Sign-problem-free QMC

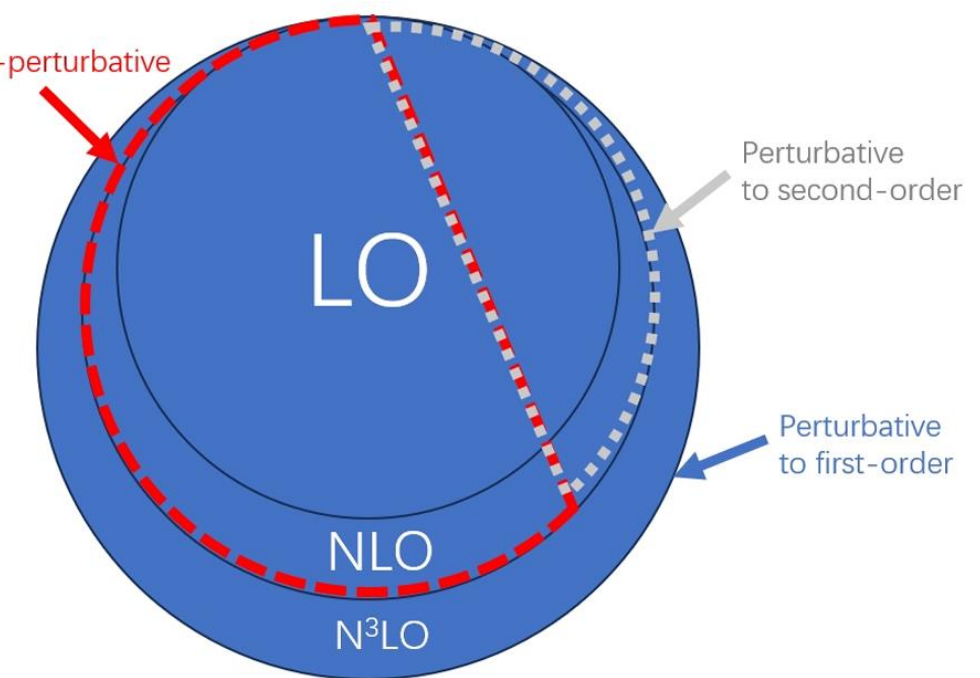
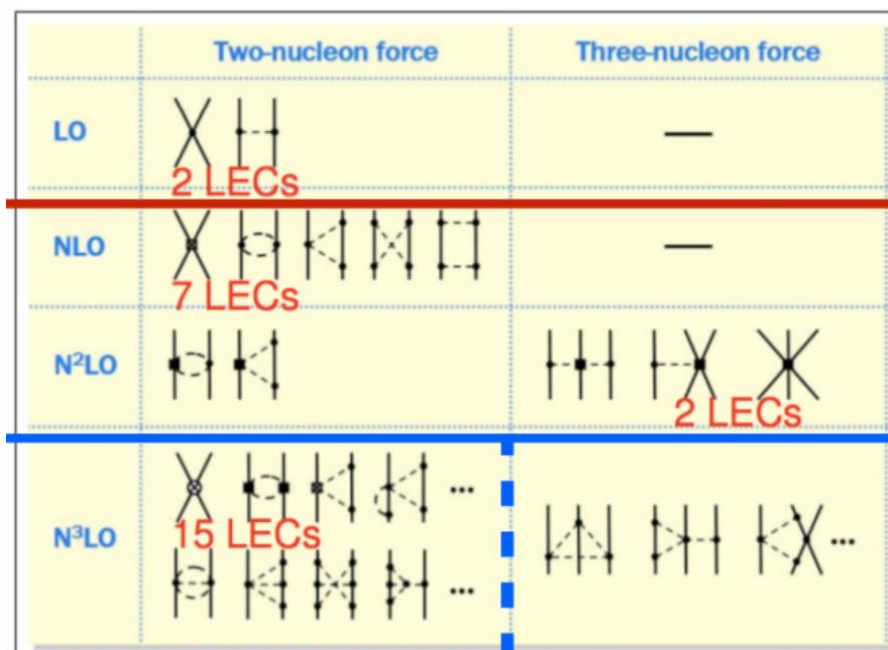
- Phenomenological interactions fitted to finite nuclei
- Scalable and unbiased, full quantum correlations ← spectrum, reaction, clustering, ...

Model	Parameterization	Parameters	σ (MeV)	Nuclei	σ_{all} (MeV)
Macroscopic-microscopic	FRDM [9]	> 30	1.15	69	0.56
Relativistic mean field	PC-PK1 [10]	11	2.25	60	1.52
Skyrme DFT	UNEDF1 [11]	12	3.43	75	1.91
Lattice EFT	Wigner-SU(4) [1]	4	10.21	55	—
Lattice EFT	LAT-OPT1	5	2.93	76	—

LAT-OPT1 has one-to-one correspondence to Skyrme force with 6 parameters except for x_0

Go beyond leading order

- Complicated structures of the nuclear forces can be included using perturbation theory

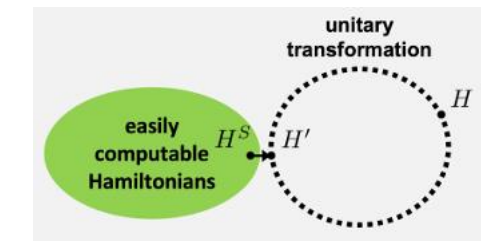


$$H_{N^3LO} = H_{SU4} + \lambda (H_{NLO} - H_{SU4})$$

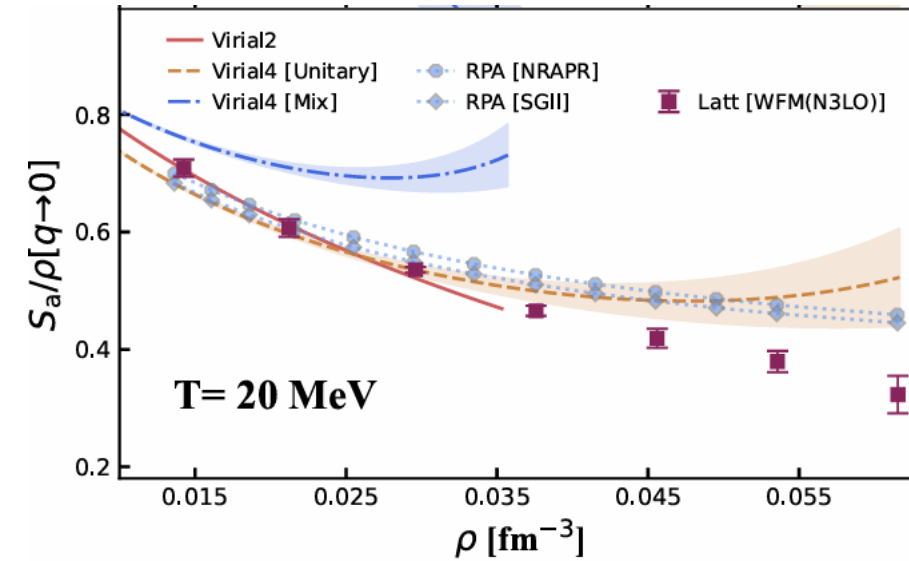
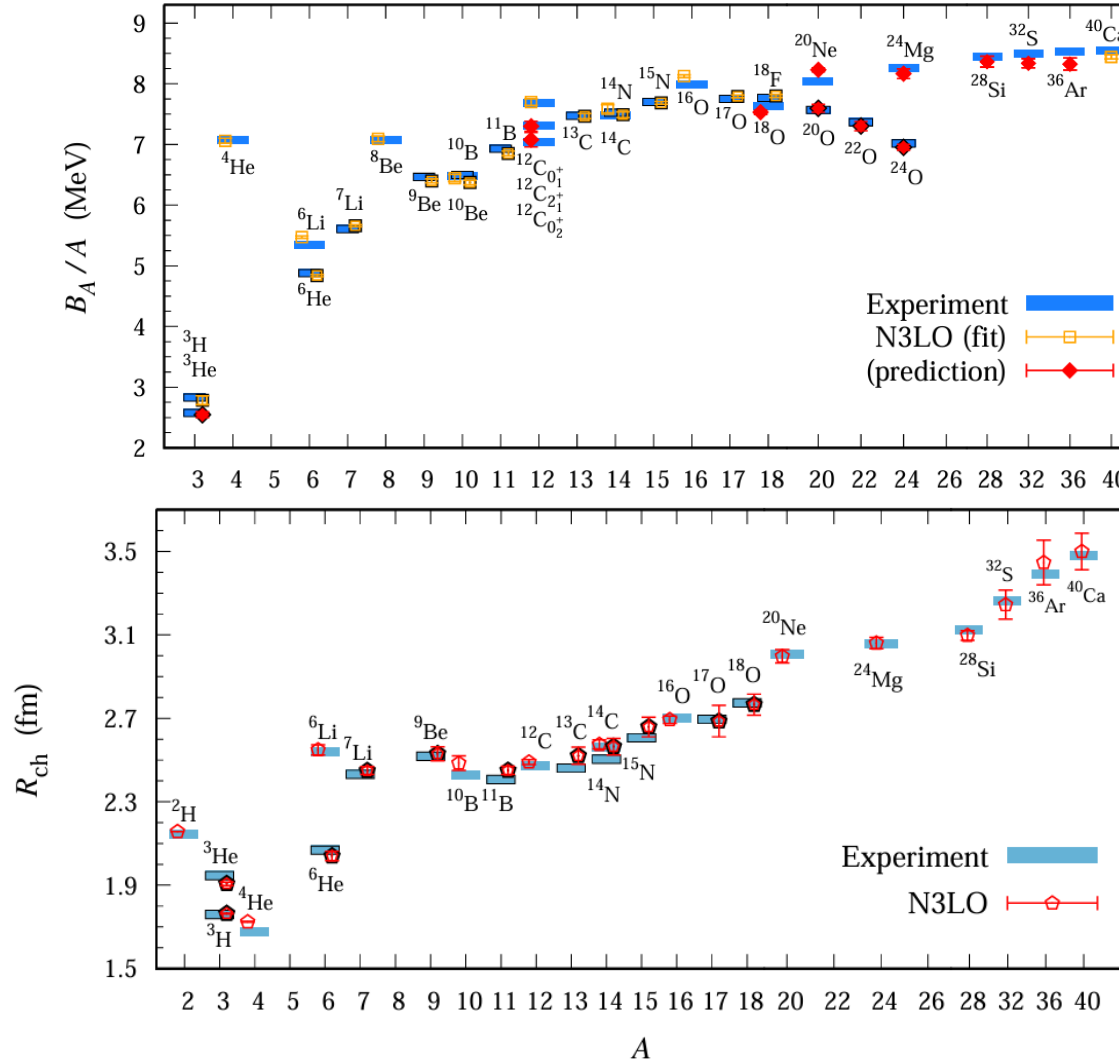
Advanced perturbative techniques

Perturbation theory can be improved with advanced algorithms

- **Perturbative quantum Monte Carlo method**, BL. et al.. PRL 128, 242501 (2022); J. Liu et al., EPJA 61, 85 (2025)
Calculate second order corrections directly
$$E_{\lambda^2} = \sum_{n>0} \frac{|\langle \Psi_0 | V_C | \Psi_n \rangle|^2}{E_0 - E_n}$$
- **Wavefunction matching method**, S. Elhatisari et al., Nature 630, 59 (2024); PRL 134, 162503 (2025); 2502.18722
Improved first order correction
- **Rank-one operator method**, Y. Ma et al., PRL 132, 232502 (2024)
Perturbatively calculate structure factors
- **Multi-channel perturbative calculations**, T. Wang et al., 2503.23840 (2025)
Perturbatively calculate beta-decay in light nuclei



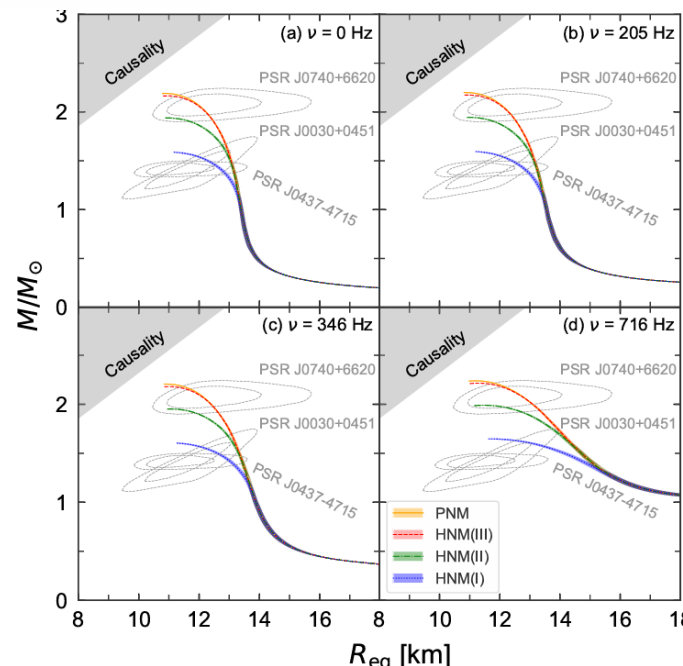
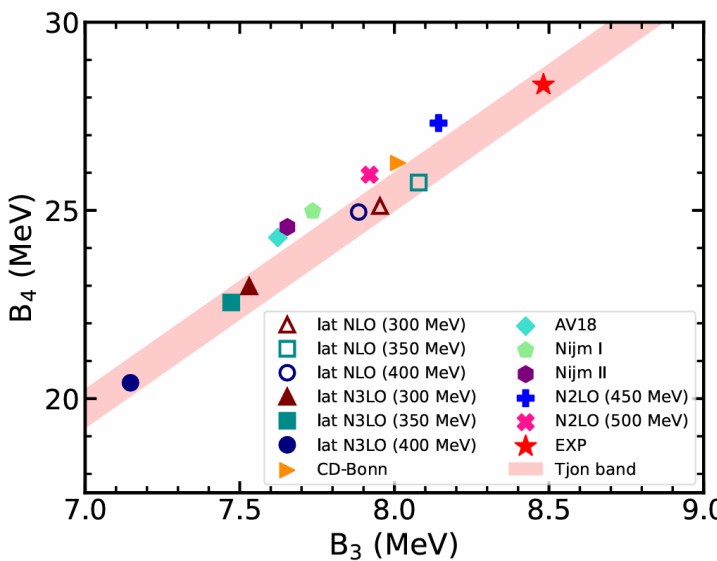
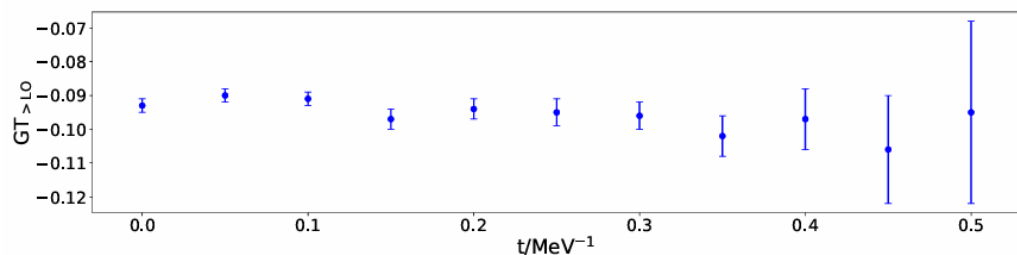
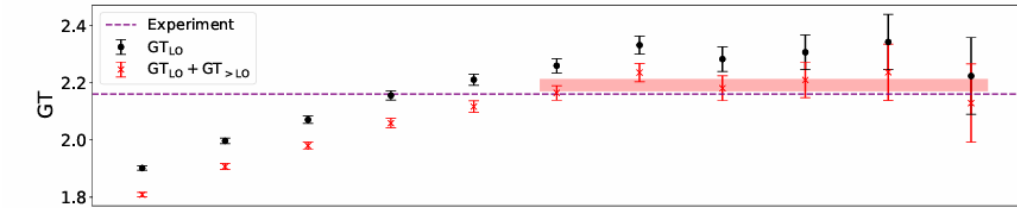
Calculations with high-fidelity nuclear forces



Calculations with N^3LO chiral forces:

- Binding energies and radii
[S. Elhatisari et al., Nature 630, 59 \(2024\)](#)
- Structure factors at finite temperature
[Y. Ma et al., PRL 132, 232502 \(2024\)](#)
- Structures of beryllium isotopes
[S. Shen et al., PRL 134, 162503 \(2025\)](#)
- Structures of carbon and oxygen isotopes
[Y. Song et al., 2502.18722 \(2025\)](#)

Calculations with high-fidelity nuclear forces



Calculations with N^3LO chiral forces
(continued):

- Hypernuclei
[F. Hildenbrand et al., EPJA 60, 215 \(2024\)](#)
- Triton beta-decay
[S. Elhatisari et al., PLB 859, 139086 \(2024\)](#)
- Structure of silicon isotopes
[S. Zhang et al., 2411.17462 \(2024\)](#)
- Hyper-neutron matter
[H. Tong et al., Sci. Bull. 70, 825 \(2025\)](#)
- DD* K three-hadron system
[Z. Zhang et al., PRD 111, 036002 \(2025\)](#)
- Correlation in light nuclei
[J. Liu et al., EPJA 61, 85 \(2025\)](#)
- Beta-decay of 6He
[T. Wang et al., 2503.23840 \(2025\)](#)

Summary and perspective

- **Sign-problem-free QMC** represents a group of **quantum many-body problems** that can be solved with **exactly polynomial scaling**. (Sign problem always induces exponential scaling)
- The **time-reversal symmetry** protect us from the **sign problem**. However, it also forbids many essential interactions (e.g. tensor force), limiting the calculations to **toy-models**.
- We firstly implement a **sign-problem-free spin-orbit term**, fit parameters to **nuclear binding energies**. The resulting nuclear force is similar to the original Skyme force, but **exactly solvable**.
- It is promising to apply the methodology from **mean-field** and **density functional theories** to improve the interactions. Our results might also provide hints connecting *ab initio* calculations and **established phenomenological models**.

Thank you for your attention!